Solar Energy 210 (2020) 128–148

Contents lists available at ScienceDirect

Solar Energy

journal homepage: www.elsevier.com/locate/solener

State-of-the-art power electronics systems for solar-to-grid integration

Venkata R. Vakacharla[a], K. Gnana[b], P. Xuewei[c], B.L. Narasimaharaju[d], Mangu Bhukya[e], Atanu Banerjee[f], Renu Sharma[g], Akshay K. Rathore[a,*]

[a] Concordia University, Montreal, QC, Canada
[b] University of Houston, TX, USA
[c] Harbin Institute of Technology, Shenzhen, PR China
[d] National Institute of Technology, Warangal, India
[e] Osmania University, Hyderabad, India
[f] National Institute of Technology, Shillong, India
[g] Shiksha 'O' Anushandhan (SOA) University, Bhubhneswar, India

A B S T R A C T

Power generated by PV panels is highly vulnerable to uncertain weather conditions, and impedance connected to its terminals. Therefore, to maximize the energy productivity from panels by controlling output impedance, a power electronic converter capable of adopting maximum power point tracking (MPPT) technique is required. This paper includes a comprehensive review of basic and advanced MPPT techniques proposed to address the variations in temperature, irradiance, partial shading conditions.

Power processing equipment such as dc/dc converters and inverters are mandatory in extracting power from PV panels and utilizing either for standalone systems or grid integration. Grid integration is a major focus where access to utility line ranging from domestic micro-inverters (< 300 W) to solar generation (> MW). A centralized inverter topology interfaces a MW power rating PV farm consisting several parallel strings of series connected PV panels to the grid. This review article contributes on presenting an overview of the state-of-the-art power electronics systems for integration of PV panels to the grid. Various interfacing power electronic architectures covering micro-inverter, central inverter up to modular inverter approach operating at low switching frequency and high switching frequency with resonant and pulse-width modulated (PWM) soft-switching or hard-switching are reported. Various voltage-fed and current-fed multi-level inverters for such architectures are studied and discussed.

1. Introduction

Solar cells, which generate electrical energy under sunlight, on connecting in series–parallel results in solar photovoltaic (PV) modules. Array configurations of PV systems are generally categorized into central, string, multistring string, and module structures. The multistring PV system is a two-stage configuration, which consists of multiple dc/dc converter interfacing each PV string and a common string inverter. For the application sensitive to the shadowing effects or PV module mismatch, module configurations are introduced. Module configuration integrates power conversion stage directly to the PV modules. Depending on the type of power conversion, module configurations are classified into cascaded dc Module (Walker and Sernia, 2004), parallel dc Module (Liu et al., 2011), ac module (Islam et al., 2006), and quasi-ac module (Rooij et al., 2015) as shown in Fig. 1.

The solar PV power can either be delivered directly by injecting the power into the utility grid by solar-to-grid integration or by operating them in islanded mode to supply power to local loads in case of remote locations. It can also be used with other energy systems such as fuel cells and energy storage (batteries, supercapacitors, flywheels) to form a hybrid energy system (Xu et al., 2018). In all the cases, the power electronic converters play an important role as shown in Fig. 2 to (1) extract maximum power from the PV panel to deliver to the load known as maximum power point tracking (MPPT) controller. (2) elevate the PV voltage to a required voltage level by a dc/dc converter and (3) convert in the ac form by a dc/ac inverter.

A major challenge in solar power system is to tackle its nonlinear current–voltage (I–V) characteristic, which results in a unique maximum power point (MPP) on its power–voltage (P–V) curve. The power generated from a given PV module mainly depends on solar insolation and panel temperature and vary with weather conditions.

Fig. 3 shows the variation of solar panel current and power with variation in solar irradiance. The panel voltage remains nearly constant; however, the panel current varies causing the change in power and so obviously the MPP. As the solar irradiance goes low, the panel current and power along with MPP goes down.

* Corresponding author at: 1455 De Maisonneuve Blvd. W., EV 5.139, Department of Electrical and Computer Engineering, Concordia University, Montreal, QC H3G 1M8, Canada.
E-mail address: akshay.rathore@concordia.ca (A.K. Rathore).

https://doi.org/10.1016/j.solener.2020.06.105
Received 13 January 2020; Received in revised form 28 June 2020; Accepted 29 June 2020
Available online 16 July 2020
0038-092X/

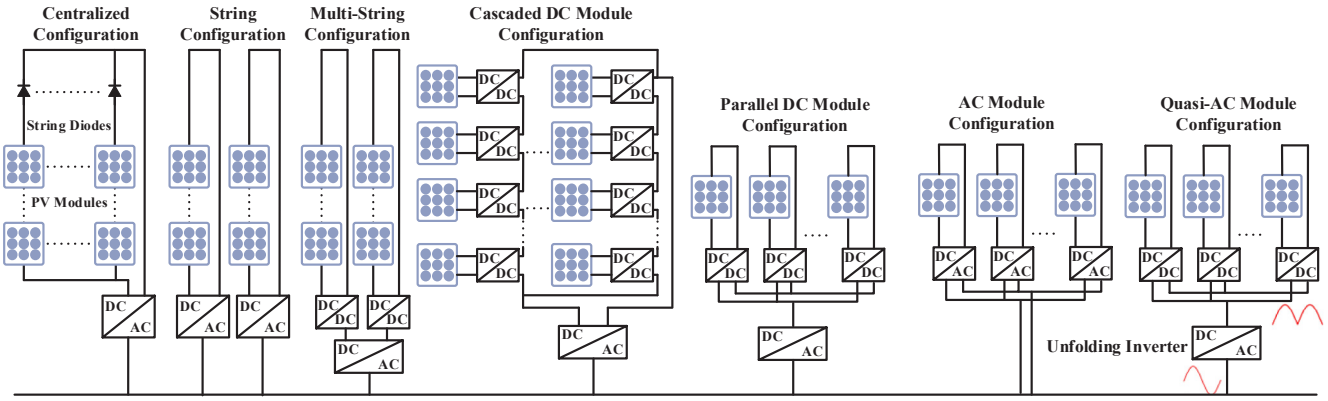

Fig. 1. Different structures used in PV system (Walker and Sernia, 2004).

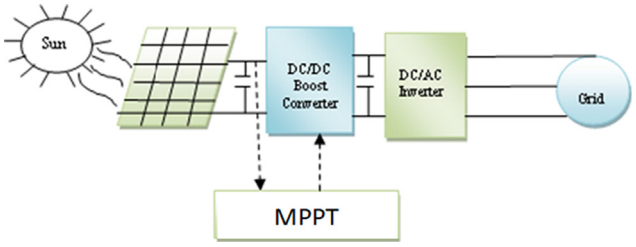

Fig. 2. Solar integrated PV conversion system with MPPT.

Fig. 4 shows the variation of solar panel voltage and power with variation in temperature. The panel current remains nearly constant; however, the panel voltage varies causing the variation in power and so obviously the MPP. As the temperature increases, the panel voltage and power along with MPP goes down.

It is essential to develop a MPPT algorithm to extract maximum power from the PV module in real time. Over the past decades, many MPPT algorithms have been proposed and discussed in the next section.

A power electronic dc/dc converter (Fig. 2) is required to implement the algorithm to physically match the load impedance with the panel impedance for maximum power transfer or to operate at the MPP.

2. MPPT techniques

MPPT is essential in solar energy system in order to harvest and deliver the maximum power to the load based on the instantaneous atmospheric conditions and requires the array voltage and current as shown in Fig. 2. Usually, in MPPT techniques, two objectives/merits are usually considered: (1) number of sensors (usually two sensors are required and one sensor or sensor-less is a merit) and (2) accuracy/oscillation at MPPT point. Additional merit can be response (fast/slow) time for reaching the MPPT point but that is associated with second merit. These are also relevant terms how the authors are using. Numerous MPPT techniques have been reported in literature for solar systems and have been classified systematically as follow:

A. Conventional techniques

Conventions MPPT techniques are the basic algorithms used and implemented widely as traditional or classical methods in early age of solar inverters. These techniques are mainly classified into four techniques.

1. Perturb and observe (P&O) method (Killi and Samanta, 2015)

   In this method the controller adjusts the voltage by a small amount from the array and measures power; if the power increases, further adjustments in that direction are tried until power no longer increases. This is called the perturb and observe method and is most common, although this method can result in oscillations of power output. It is referred to as a 'hill climbing' method, because it depends on the rise of the curve of power against voltage below the MPP, and the fall above that point. Perturb and observe is the most commonly used MPPT method due to its ease of implementation.

2. Incremental conductance (IC) method (Liu et al., 2008; Elgendy et al., 2012)

   IC method has a better performance compared to the P&O method because it has succeeded in minimizing the oscillations around the MPP point. The IC can determine that the MPPT has reached the MPP and stop perturbing the operating point. If this condition is not met, the direction in which the MPPT operating point must be perturbed can be calculated using the relationship between dI/dV and –I/V This relationship is derived from the fact that dP/dV is negative when the MPPT is to the right of the MPP and positive when it is to the left of the MPP.

3. Constant voltage MPPT method (Leedy et al., 2012; Aganah and Leedy, 2011)

   A constant voltage MPPT algorithm that automatically adjusts the reference voltage to account for varying environmental conditions. The solar array source is configured such that its open-circuit voltage is sampled without breaking the entire source from the load as is the case with other constant voltage MPP algorithms.

4. Open circuit method (Bharath and Suresh, 2017; Lopez-Lapena and Penella, 2012)

   In this MPPT method, the solar array is disconnected periodically to sample the open circuit voltage of the solar panel and then use its value for MPPT. It's an approximate MPPT method.

B. Predictive techniques

Predictive models use known results to develop (or train) a model that can be used to predict values for different or new data. The modeling results in predictions that represent a probability of the target variable based on estimated significance from a set of input variables. Predictive models are used to find potentially valuable patterns in the data, or to predict the outcome of some event.

Two predictive MPPT techniques used for solar MPPT are as follow:

1. Dual-Discrete model predictive control (Lashab et al., 2019)

   This method presents a method that overcomes the problem of the confusion during fast irradiance change in the classical maximum power point tracking (MPPT) as well as in model predictive control (MPC)-based MPPTs available in the literature. The model of the photovoltaic (PV) array is also considered also in addition to the converter model in the proposed algorithm, which allows it to be prompt during rapid environmental condition changes.

2. Sensorless current-based model predictive control (Metry et al., 2016)

   The main contribution of this technique is the use of model-based

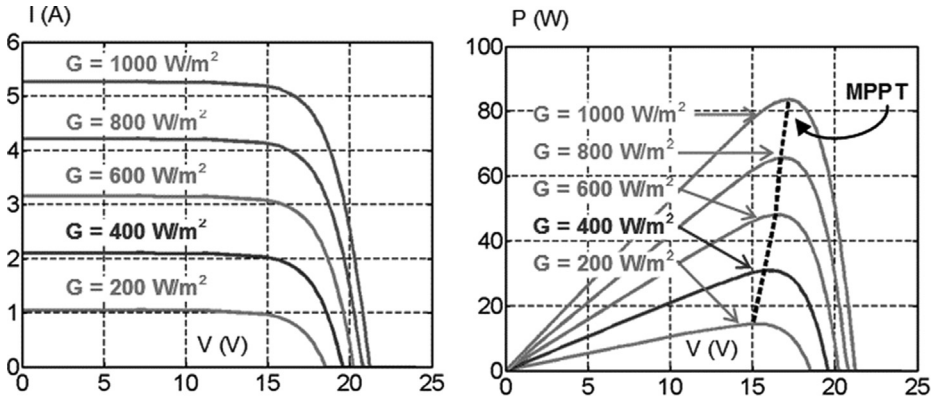

Fig. 3. Variation in solar panel current and power with variations in solar irradiance.

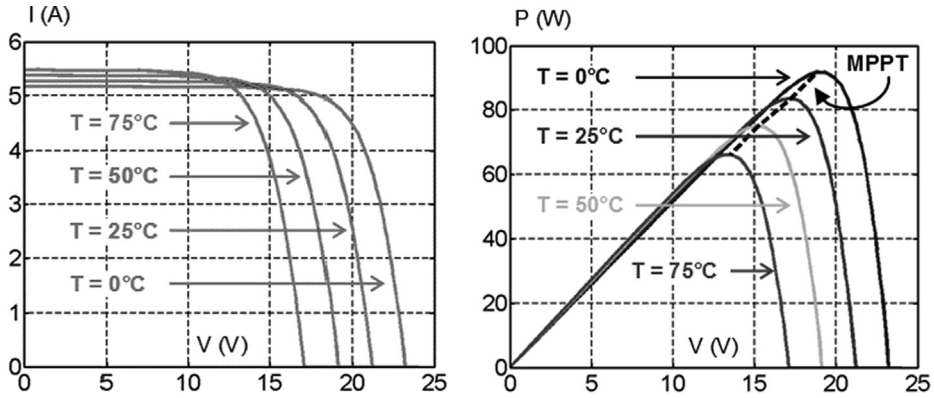

Fig. 4. Variation in solar panel voltage and power with variations in temperature.

predictive control principle to eliminate the current sensor that is usually required for well-known MPPT techniques such as P&O. By predicting the PV system states in horizon of time, the proposed method allows faster response and lower power ripple in steady state than the conventional P&O technique under rapidly changing atmospheric conditions.

C. Artificial Intelligence (AI) Techniques

Artificial intelligence is the ability of a computer system or actual complex algorithms to estimate relationships of the complex datasets and also to find correlations, which may result into testable hypotheses. The technique can be introduced to MPPT calculation algorithms too. The following AI MPPT techniques have been reported for MPPT:

1. Artificial neural network techniques (Lin et al., 2011):
   To achieve a fast and stable response for the real power control, the intelligent controller consists of a radial basis function network (RBFN) and an improved Elman neural network (ENN) for maximum power point tracking (MPPT).
2. Fuzzy logic control (Larbes et al., 2009):
   A fuzzy logic controller based MPPT (FLC) is then proposed which has shown better performances compared to the P&O MPPT based approach. The proposed FLC has been also improved using genetic algorithms (GA) for optimization.
3. Genetic algorithm control (Daraban et al., 2013):
   This algorithm is used for searching the global maximum power point (GMPP) for photovoltaic systems affected by partial shading. The P&O algorithm is embedded into the GA function for improving the optimization process. By adding this functionality to the algorithm, the number of iterations and the population size is low, thus finding the MPP in a short time.

D. Meta Heuristic Optimization techniques

A wide range of metaheuristic algorithms have emerged over the last two decades, and many metaheuristics such as particle swarm optimization (PSO) are becoming increasingly popular. Despite their popularity, mathematical analysis of these algorithms lacks behind. Convergence analysis still remains unsolved for the majority of metaheuristic algorithms, while efficiency analysis is equally challenging.

Optimization techniques based basic and popular MPPT techniques are as follow:

1. PSO (Liu et al., 2012)
   Particle swarm optimization (PSO) is a population-based stochastic optimization algorithm motivated by intelligent collective behavior of some animals such as flocks of birds or schools of fish. Since presented by Kennedy and Eberhart in 1995, it has experienced a multitude of enhancements. This method performs the search of the optimal solution through agents, referred to as particles, whose trajectories are adjusted by a stochastic and a deterministic component.
2. ARMO based MPPT technique (Seyedmahmoudian et al., 2019)
   This study aims to design, develop, and verify a novel rapid, reliable, and cost-effective method called adaptive radial movement optimization (ARMO) to diminish the effect of the partial shading problem in the MPP detection for PV systems with additional dynamic applications. The main advantages of ARMO are its improved tracking speed and significant reduction in output fluctuations during the tracking period.
3. Grey Wolf optimization (GWO) (Mohanty et al., 2015):
   The GWO is a new optimization method which overcomes the limitations such as lower tracking efficiency, steady-state oscillations, and transients as encountered in P&O. It showed better performance under partial shading conditions compared with P&O.

E. Modified and improved techniques

With time, several of existing classical techniques were either modified to improve the accuracy and performance under variance of irradiance and partial shading. Some of the modified MPPT techniques with improved performance have been renamed and presented as follow:

1. Modified P&O with reduced oscillation (Ahmed and Salam, 2016):
   The modified scheme retains the conventional P&O structure, but with a unique technique to dynamically alter the perturbation size. At the same time, a dynamic boundary condition is introduced to ensure that the algorithm will not diverge from its tracking locus.
2. Improved performance low-cost IC PV MPPT technique (Zakzouk et al., 2016):
   An enhancement is introduced to IC algorithm in order to entirely eliminate the division calculations involved in its structure. Hence, algorithm implementation complexity is minimized enabling the utilization of low-cost microcontrollers to cut down system cost. A modified variable-step size, which depends solely on PV power, is proposed. It achieves enhanced transient performance with minimal steady-state power oscillations around the MPP even under partial shading.
3. Enhanced adaptive P&O (EA-P&O) (Ahmed and Salam, 2018):
   The objective is to mitigate the limitations of the conventional P&O namely, the steady-state oscillation, diverged tracking direction, and inability to detect the global peak during partial shading. A smart oscillation detection scheme and a dynamic boundary condition resolve the first two problems, respectively. Meanwhile, an intelligent prediction method is designed to ensure that the global peak is always correctly tracked. Another feature is the open-circuit voltage is determined without using sensors.

F. Hybrid MPPT Technique such as

1. Grey Wolf-Assisted P&O (Mohanty et al., 2016)
   This paper proposes a new hybrid maximum power point tracking (MPPT) algorithm combining grey wolf optimization (GWO) and perturb & observe (P&O) technique for efficient extraction of maximum power from a photovoltaic system subjected to rapid variation of solar irradiance and partial shading conditions. GWO handles the initial stages of MPPT followed by application of the P&O algorithm at the final stage in view of achieving faster convergence to the global peak (GP). This MPPT thus overcomes the computational overhead as encountered in the case of a GWO-based MPPT algorithm. The idea behind using the hybrid technique is to scale down the search space of GWO which helps to speed up for achieving convergence toward the GP.

G. Miscellaneous techniques

Additional popular, efficient and effective techniques used for solar MPPT are as follow:

1. Based on an image of PV modules (Mahmoud and El-Saadany (2016))
   A new MPPT technique is proposed in this paper that is distinguished by its ability to find the global maximum power peak (GMPP) without the need for periodic curve scanning. The proposed method utilizes the mathematical model of the PV module, as well as the irradiances received by its PV cells, to analytically calculate the location of the GMPP. The required irradiances are innovatively estimated using an image of the PV module captured by an optical camera. The proposed method is also combined with the perturb and observe method to compensate for errors in the model or irradiance estimation.
2. Analog BJT-Tuned MPPT (Al-Soeidat et al., 2018):
   An analog, bipolar junction transistor (BJT)-tuned voltage reference maximum power point tracking (MPPT) method for photovoltaic modules is proposed. The conventional fixed voltage reference method does not obtain good MPPT efficiency because the MPP voltage changes at different insolation levels. An approximately linear slope is formed when connecting the MPPs measured from the highest insolation level to the lowest. Utilizing this characteristic, a BJT, which has a similar electrical property, is used to implement a variable voltage reference that improves the accuracy of the MPP voltage when the insolation changes. The proposed circuit is simple and easy to implement, and it can track the MPP very quickly without the need for a digital controller or PID controller. Hence, the circuits cost and complexity are reduced.
3. Voltage-sensor-based MPPT for standalone systems through voltage reference control (Killi and Samanta, 2019):
   A single voltage-sensor-based MPPT controller with improved tracking performance is presented. The MPPT controller can be implemented by either direct duty cycle or voltage reference control in conjunction with a proportional and integral (PI) controller. The voltage reference control has the advantages of faster convergence and small oscillations in steady state compared with the direct duty cycle method. Moreover, the controller gains can be analytically calculated unlike trial-and-error-based selection of scaling factors for the direct duty cycle method. Thus, voltage-sensor-based MPPT algorithm through a voltage reference control technique with the help of the PI controller is developed for minimizing the tracking time and steady-state oscillations.

   A knowledge of the state-of-at-the-art MPP techniques (conventional to advanced) offers the researchers and the solar inverter and charge controller manufacturers about the advancement made in this field of MPPT control as well as the algorithms developed for MPPT tracking. The advancement may be in terms of cost reduction with the reduction in the number of sensors, the precision level of effectiveness in MPPT tracking to avoid oscillations around the maximum power point, and the response time (fast or slow tracking) of MPPT. This review covers from conventional to the latest advancement in MPPT control techniques. MPPT algorithms are implemented through switching power converters. Power electronics is an important enabling technologies to connect solar panels to the load with desirable load interactive power conditioning. It not only matches the source and load specifications but also enables maximum power transfer to the load along with load voltage regulation and power flow control despite varying input electrical specifications based on atmospheric conditions. In the next sections, high-frequency soft-switching dc/dc converters and low frequency multilevel inverters are discussed. Various configurations to introduce soft-switching have been reported. Both, voltage-fed and current-fed power converters have been elaborated.

3. High-frequency (HF) dc/dc converters

Dc/dc converters are usually adopted for these module-integrated converter for dc module and quasi-ac module configurations as shown in Fig. 1. Even for ac module configuration, additional dc/dc converter with HF isolation are widely used to interface low voltage PV modules. Therefore dc/dc converters play an essential role in both multistring and module configurations of PV systems.

The overall requirements of dc/dc converters for PV systems are summarized as follows: (1) high voltage gain to elevate solar panel voltage; (2) low input ripple for better MPPT tracking; (3) high efficiency for faster return on investment; (4) low cost for system commercialization, (5) low volume for space consideration, and (6) long lifetime (matching 25 years of warranty with solar panels). Galvanic isolation is also preferred to reduce the ground leakage current. Dc/dc converters can be classified into two major types, voltage-fed and current-fed. The difference is that voltage-fed converter employs a large capacitor in parallel connection with the source while current-fed converter employs an inductor in series connection with the source. The HF isolated dc/dc converters for PV system applications have emerged as possible solution for the low cost, light weight, and low volume

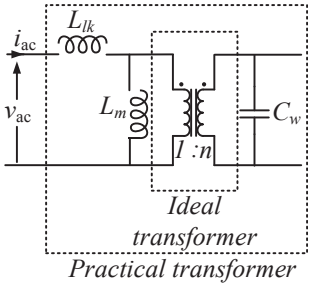

Fig. 5. Significant non-idealities in practical transformer when operated at high frequency (Johnson et al., 1988).

benefits. HF pulse width modulated (PWM) dc/dc converters and HF resonant converters are two mainstreams.

3.1. HF resonant dc/dc converters

Isolation element, the high frequency transformer, in power electronic converters for high voltage gain applications such as solar-grid integration exacerbates its non-idealities due to large turn ratio and higher switching frequency (Johnson et al., 1988). Unnegotiable leakage inductance and winding capacitance, as shown in Fig. 5, interfere with underlying operation of converter generates voltage and current spikes respectively. This increases conduction losses, switching loses thus demands bulky snubber circuits and heat sinks to maintain thermal stability (Outeiro et al., 2016).

Resonant converters offer lucrative solution to such cases (Forouzesh et al., 2017). The philosophy of resonant conversion involves engaging transformer non-idealities such as leakage inductance and winding capacitance into converter operation there by eliminating unnecessary current and voltage spikes caused by them. A properly designed resonant tank can reshape device current and voltage there by eliminating switching losses to consequentially push efficiency, switching frequency and power density further (Steigerwald, 1988). Few resonant conversation techniques allow to integrate device and diode parasitic into soft switching resonant components (Tabisz and Lee, 1991). Depending on loading, available input and converter operation, resonant converters can be broadly classified into following groups.

a. Load resonant converter, voltage fed type.
b. Load resonant converter, current fed type.
c. Quasi resonant converter, voltage fed type.
d. Quasi resonant converter, current fed type.

A. **Load resonant converters**

In this type of conversion resonant elements not only contribute for soft switch transition during switching but also participate during complete high frequency switching cycle. Therefore, characteristics of load resonant converters are highly influenced by type of resonant tank employed (Tan and Ruan, 2016; Yu et al., 2018). A basic load resonant dc/dc converter with various stages involved is depicted in Fig. 6(a). In a nut shell, operation of load resonant converter involves inversion of input dc voltage by Front End Inverter (FEI) to feed resonant tank with high frequency ac wave form. Resonant tank in turn processes and passes it onto transformer followed by Rear End Rectifier (RER) which rectifies and filters the available high frequency ac voltage to feed the dc bus. Depending on application, RER could be full wave rectifier or full bridge rectifier (Johnson et al., 1988; Yu et al., 2018).

Applications with low voltage and high current such as voltage regulators (Yang et al., 2002), by nature, favors full wave rectifier as RER with less devices for minimized voltage drop and power losses. Further synchronous rectification abates conduction losses with minimum possible (two) active switches (Johnson et al., 1988). On the other hand high voltage and low current applications such as solar–grid integration, by nature go with full bridge rectifier as RER. Further RER allows to extend full bridge in to voltage doublar and quadrapular configurations (Yu et al., 2018). Also, operating resonant converter above resonance manifests zero voltage switching (ZVS) switching and below resonance results in zero current switching (ZCS) operation (Steigerwald, 1988).

(1) Voltage fed type

In this type of converters, FEI is directly driven by voltage source which is responsible to supply high harmonic switching current to resonant converters. Such converters when used in connection with PV needs bulky electrolytic capacitor rated at input voltage to supply high harmonic ripple current which extends PV life time.

In a half bridge series resonant converter (FEI, Fig. 6(b1); Resonant tank, Fig. 6 (c1)), interestingly, resonant capacitor appears in series to transformer helps blocking dc voltage to prevent transformer from flux walking (Tan and Ruan, 2016). Also, currents through switches are in proportion with load currents offers acceptable light load efficiency. But limited selectivity of the resonant tank complicates light load operation. Therefore, series resonant converters cannot offer wide load variation as required by solar-grid integration. Further, frequency modulation is another major drawback (Vorperian and Cuk, 1982; Oruganti and Lee, 1985a, 1985b). Further, high voltage gain demand by grid integration and step-down nature of FEI pushes up transformer turns ratio.

Solar-grid integration demands higher power densities. Therefore, operating a converter at a fixed frequency helps to optimize the magnetic design, control circuitry and EMI filters (Pitel, 1986). Therefore clamped mode series resonant converter with full bridge FEI, which operates under fixed switching frequency, is more suitable for solar-grid integration rather than half bridge FEI (Agrawal et al., 1989; Sabate and Lee, 1991; Tsai and Lee, 1988; Tsai et al., 1988).

Resonant inductor appears in series to leakage inductance of practical transformer, but winding capacitance is not included into converter operation. Therefore, for every high frequency voltage reversal in resonant tank, none of the RER diodes are forward biased for power transfer unless parasitic capacitor (C_w) is charged/discharged. This abnormal subinterval hinders the power flow and increases output current ripple. Therefore, voltage-fed series resonant converters need overdesigned output filter capacitor for solar-grid integration (Johnson et al., 1988).

On the other hand, a half bridge parallel resonant converter (FEI, Fig. 6 (b1); Resonant tank, Fig. 6(c2)) integrate both leakage inductance and winding capacitance into converter operation (Ranganathan et al., 1982; Bhat and Swamy, 1989; Steigerwald, 1984). However, output LC filter turns as bulky as transformer in case of high output voltage applications such as solar-grid integration. Therefore, both series and parallel resonant converters suffer from bulky output filter. However lower currents on secondary side can increase resonant capacitor life time and thus reliability of the converter (Tan and Ruan, 2016). Further, this converter offers inherent short circuit protection. However, energy stored in resonant tank is independent of load current. Therefore, light load efficiency is poor (Steigerwald, 1988).

Unlike half bridge parallel resonant converter, full bridge counterpart (FEI: Fig. 6(b2)) offers fixed switching frequency operation as required by solar-grid integration (Tsai et al., 1989). However, parallel resonant converter is devoid of series capacitance which exposes transformer to risk of flux walking.

Drawbacks of series (inability to regulate under no load) and parallel (independence of stored resonant energy on load) resonant converters are alleviated in half bridge series–parallel resonant converter (FEI, Fig. 6(b1); Resonant tank, Fig. 6(c3)) which could be a suitable candidate for solar-grid integration (Bhat and Dewan, 1987).

It carries advantages of both series and parallel resonant converters.

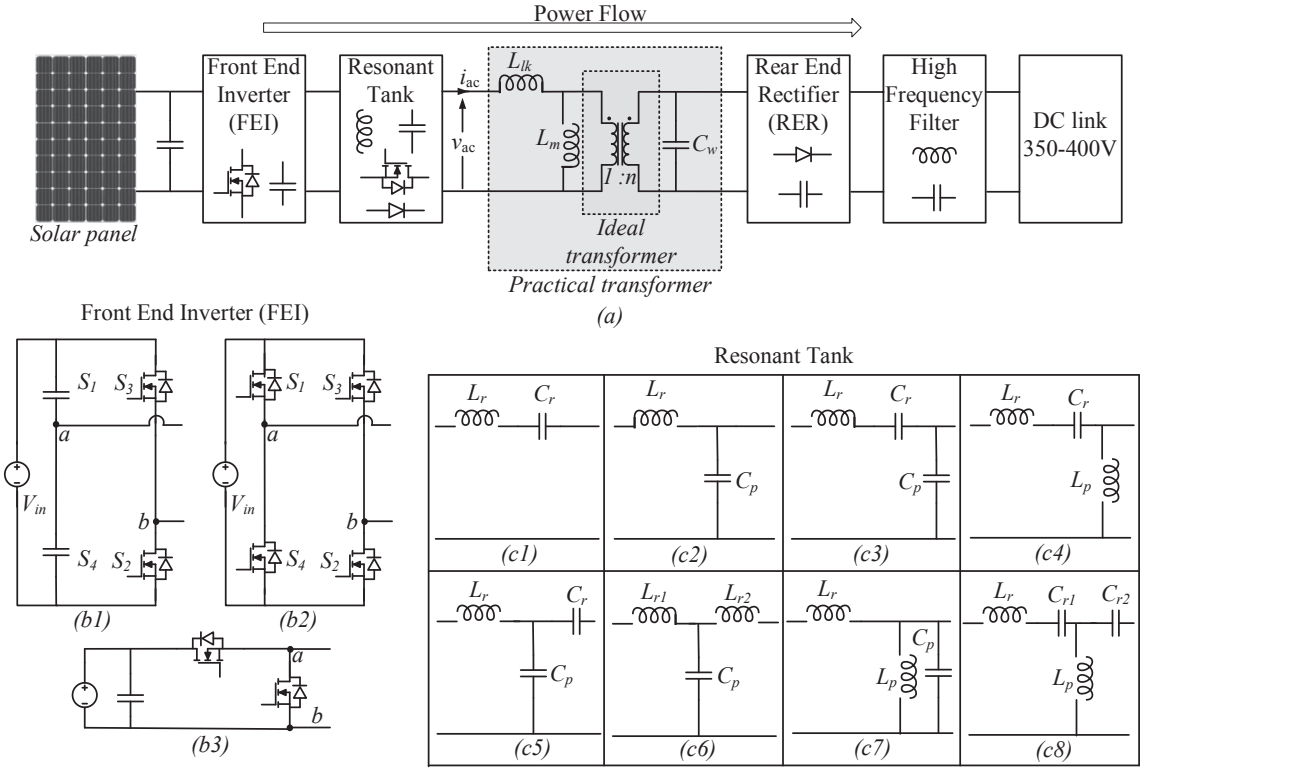

Fig. 6. (a) Block diagram of resonant converters. (b1) Half bridge FEI, (b2) Full bridge FEI, (b3) Class-D FEI, (c1) Series resonant tank, (c2) parallel resonant tank (c3) series parallel (LLC) resonant tank (c4) LLC-SRC (c5) LCC-T resonant tank (c6) LCL-T resonant tank (c7) (LC)(LC) resonant tank (c8) (LC)LC resonant tank.

However, bulky LC filter in output, wide range frequency operation and compromised light load efficiency remain major drawbacks of this converter. Even though LC filter can be replaced with capacitive filter (Biela et al., 2009; Martin-Ramos et al., 2007, 2008; Sewell et al., 2003; Ivensky et al., 1999), variable frequency operation is checked with clamped voltage capacitance method (Bhat, 1992, 1995a,b; Garcia et al., 1994), domination of parallel resonant tank characteristics deteriorate light load efficiency.

Another half bridge LLC-SRC resonant converter (FEI, Fig. 6(b1); Resonant tank, Fig. 6(c4)), a modified version of series resonant converter, is studied with an intention to alleviate drawbacks of series resonant converter i.e., light load regulation sensitivity (Bhat, 1990). LLC-SRC resonance tank is formed by placing an inductor in parallel to transformer of a series resonant converter. Such a modified resonant tank gain characteristics have load independent gain near ZVS region and thus needs minimum variation in frequency for load compensation. Similar to series resonant converter, resonant capacitor (C_r) can block dc voltage into transformer. A constant frequency LLC-SRC resonant converter (FEI, Fig. 6(b2); Resonant tank, Fig. 6(c4)) are given in (Bhat, 1995a,b; Bhat, 1997; Borage et al., 2005, 2007). Further enhancement in voltage conversion ratio, extend input and load range is achieved by split LLC-SRC resonant tank as shown in Fig. 7 (Sun et al., 2018). Four

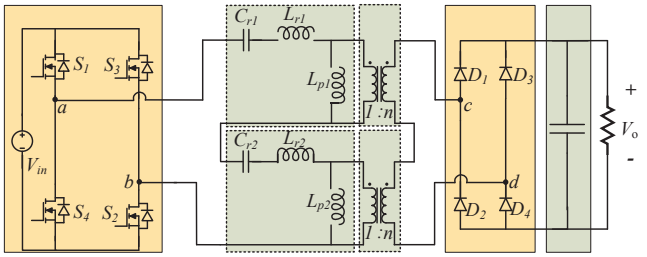

Fig. 7. Voltage fed split LCC-SRC resonant converter for wide input voltage and load disturbances.

element based resonant converters are also analyzed (Bucher and Duerbaum, 2010; Shafiei et al., 2011) for better performances.

Design and optimization of above resonant converters against load fluctuations is not easy due to load dependent resonant tanks. A simple two-stage, buck followed by voltage fed push pull resonant converter is proposed in (Blanes et al., 2011). Front end buck stage compensates load and input fluctuations to decouple its influence on frequency of operation. On the other hand, voltage fed push pull load resonant converter needs very simple gate drive needs as opposed to (Boonyaroonate and Mori, 2002; Ryan et al., 1998; Chu and Li, 2009). Further, it offers fixed frequency of operation and for load and input range.

However, inherently voltage fed resonant converters demand bulky electrolytic capacitor rated at maximum input to enhance life time of PV panel. But it limits life time of converter relative to PV panel life. Fortunately current fed converter offer suitable compact solution.

(2) Current fed type

Current fed converters adopt inductive input filter which smoothen input current ripple and enhances reliability of converter. Popular duality technique is instrumental in deriving current fed converter topologies from well-established and verified voltage fed converters. Depending on nature of switching device, the current fed converters are classified as converters with unidirectional voltage blocking switches and bi-directional voltage blocking switches (Kazimierczuk and Abdulkarim, 1995; Sasmal and Sensarma, 2018; Vishal et al., 2018). Converters (Kazimierczuk and Abdulkarim, 1995; Sasmal and Sensarma, 2018; Vishal et al., 2018) obtained by applying duality principle to each operating mode of respective voltage fed converter counterpart; on the other hand, current-fed converter can also be obtained by applying duality principle to each stage (Wolfs, 1993).

(a) Bidirectional voltage blocking switches

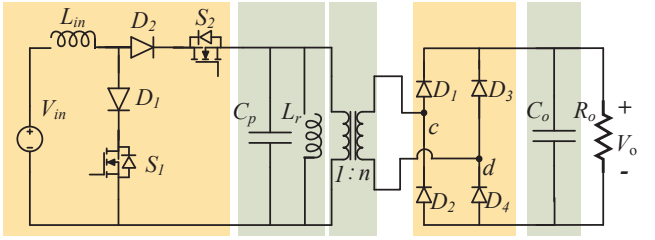

Fig. 8. Class-D current source parallel resonant converter using bidirectional voltage blocking switch.

A simple bidirectional voltage blocking switch based class-D current source parallel resonant converter, as shown in Fig. 8, with comprehensive analysis and design is presented in (Kazimierczuk and Abdulkarim, 1995). Full bridge FEI with similar switches, as shown in Fig. 9(a), is presented in (Sasmal and Sensarma, 2018; Vishal et al., 2018). (LC)(LC) resonant tank and LC resonant tank are adopted in (Sasmal and Sensarma, 2018; Vishal et al., 2018) respectively. A bidirectional voltage blocking switch is achieved by series connection of diode and MOSFET such that series diode disables body diode of MOSFET. Such diodes carry complete load current and not suitable for solar-grid integration as they compensate recovered switching losses with blocking diode conduction losses. This worsens with full bridge configuration. Further, optimization of magnetics and control circuitry is not possible due to variable frequency operation (Sasmal and Sensarma, 2018; Vishal et al., 2018).

(b) Unidirectional voltage blocking switches

On the other hand, a basic current fed converter with unidirectional voltage blocking switches (MOSFET) includes cascaded boost converter followed by unregulated voltage fed class-D LLC-SRC resonant converter (Kim et al., 2013) or a push pull resonant converter (Barbi and Gules, 2003). Front end boost converter compensates load and input disturbances and operates converter at fixed frequency at the expense of higher conduction losses. Push-pull converter (Thrimawithana and Madawala,2008) eliminates front end buck converter, but operates at variable switching frequency. A fixed frequency current fed push–pull (Kim and Kwon, 2009; Kwon et al., 2009a,b) load resonant converter adopts clamped switches. However, high side switches complicates driving scheme and raises component count, power losses in converter. By shifting active-clamp onto input inductor (Wu et al., 2017) maintains all merits offered by (Kim and Kwon, 2009).

Active clamped interleaved boost converters based FEI (Fig. 9(b)), two LLC resonant tanks, each connected to one boost converter, is presented in (Lin and Lin,2019) operates in variable frequency mode with zero input current ripple. Like (Lin and Lin, 2019), converter presented in (Shang et al., 2017) as shown in Fig. 10 needs high component count but operates on fixed frequency and maintains soft

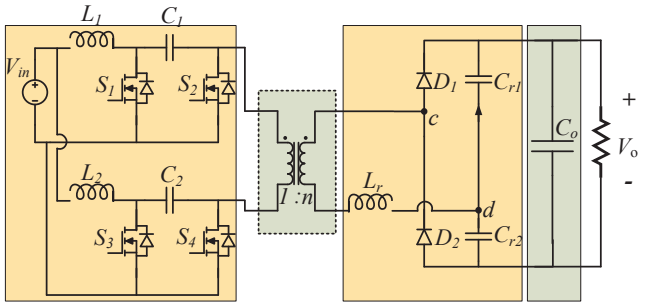

Fig. 10. Current fed load resonant converter (54).

switching against wide input and load disturbances. However, (Patti et al., 2014; Rathore et al., 2016; Vakacharla et al., 2018; Vakacharla and Kumar Rathore, 2018, Vakacharla and Rathore, 2019a, 2019b, 2019c) adopt simplest of FEI (Fig. 9(c)) to maintain less component count and soft switching in all devises under wide input and load disturbances. Current fed resonant converter with LCC-T resonant tank, exhibit ZVS, and operate with variable switching frequency and duty ratio (hybrid control) (Vakacharla and Rathore, 2019a). On the other hand, same converter on operating with fixed frequency exhibit ZCS turnoff (Vakacharla and Rathore, 2019c). Similarly, converters adopt LCC tank (Patii et al., 2014), LCL-T tank (Rathore et al., 2016), LLC-SRC tank (Vakacharla and Rathore, 2019b) and LCL resonant tank (Rathore et al., 2016) successfully operate with constant switching frequency, constant input current, wide load range and input operation in favor of solar-grid integration. However, clamp capacitors in FEI reduces reliability of converter.

(3) Steady state and dynamic modelling

Steady state modelling of resonant converters is inherently complex due to higher number of state variables. Conventional techniques such as time domain (Lee and Siri, 1986; Gilbert et al., 2007, Bhat, 1991 state-space (Kang et al., 1991; Martin-Ramos et al., 2007) and state-plane (Lee and Siri, 1986) approaches proved to be laborious and frustrating engineers to explore. Fundamental Harmonic Approximation (FHA) analysis reduces resonant converter into Equivalent Linear Sinusoidal (ELS) circuit which avail simple fundamental ac analysis techniques for mathematical modelling. To match solar-grid integration requirements, parallel and series–parallel resonant converters operate with capacitive filter instead of bulky LC filter. Such modifications further complicates the operation and modeling of converter with discreet resonance. FHA technique also turns complex in such cases (Bhat, 1992; Sewell et al., 2003) thus (Vakacharla and Rathore, 2019a) presented technique to restore simplicity of FHA. A comparison of FHA techniques pertaining to accuracy and complexity in case of full bridge series–parallel resonant converter with capacitive output filter is

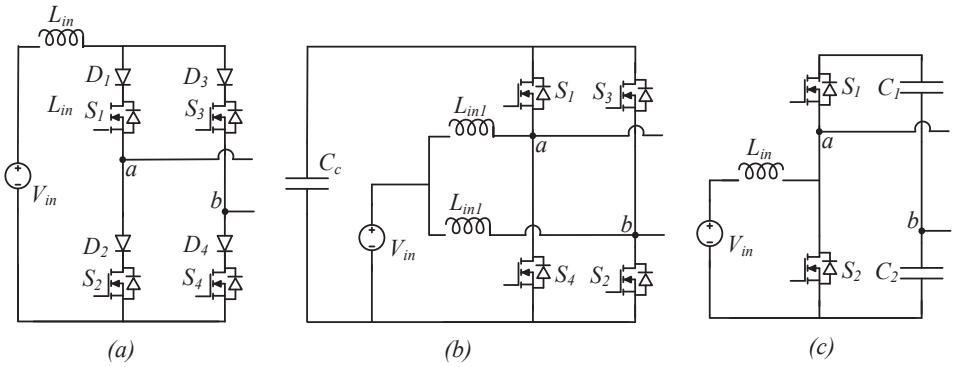

Fig. 9. FEI with (a) Full bridge (bidirectional voltage blocking switches) (b) Active clamped dual boost (c) Active clamped boost.

Table 1
Comparison of proposed technique with various techniques proposed in literature.

	Bhat (1992)	Sewell et al. (2003)	Ivensky et al. (1999)	Vakacharla and Kumar Rathore (2018)
ELS Circuits	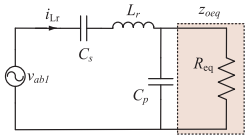	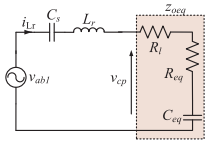	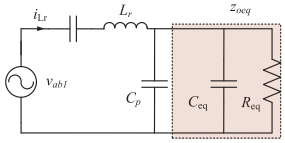	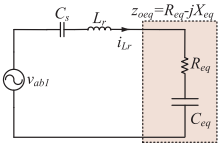
z_{oeq}	(2)	(3), (4), (5)	(6), (7), (8), (9)	(1)
Accuracy	Highly inaccurate	Accurate	Moderately accurate	Accurate
Solution type	Closed	Unclosed; (5)	Closed	Closed
Complexity	Simple	Requires numerical methods	Requires curve-fitting methods.	Simple

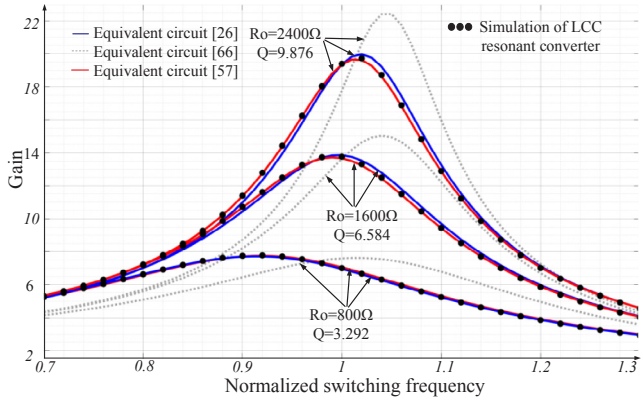

Fig. 11. Comparison of voltage gain predicted by ELS circuit (Ivensky et al., 1999; Rathore et al., 2016; Bhat, 1992) with voltage gain obtained through simulation of actual LCC resonant converter.

presented in Table 1. Also, a comparison of gain predicted ELS models derived by various FHA methods is presented in Fig. 11. Similarly, (Bhat, 1992) details about modelling of LLC-SRC resonant converter.

Solar-grid integration expects a regulated dc bus against all odds to feed grid-connected inverter. Therefore, dynamic model of the converter for controller design is necessary. Dynamic models obtained from discreet time-modelling approach (Verghese et al., 1986; Vorperian and Cuk, 1983) lack in universality, simplicity and insight in dynamic operation. Inspired from FHA, Extended Describing Function (EDF) (Martin-Ramos et al., 2007; Yang et al., 1992; Tian et al., 2016; Hsieh and Lee, 2018a) dynamic models can consider significant harmonic orders, apart from fundamental, in resonant tank, thus universal. However, complex in approach. Another approach, rotating co-ordinate method allows perturbation and linearization valid in case of resonant converters (Hsieh and Lee, 2018b). An accurate state plane approach is detailed in (Hsieh and Lee, 2018a).

B. Quasi resonant converters

In quasi-resonant converters resonant elements contribute only for soft switch transition during switching. Conventional switches, in combination with auxiliary reactive elements, can be forced to carry quasi-sinusoidal currents and/or voltages to eliminate switching losses (Tabisz and Lee, 1991). Such switches are called resonant switches. Replacing conventional switches of PWM converters with such resonant switches results in quasi-resonant converters. As an example, Quasi resonant ZVS (resonant capacitor is in parallel with device) switching buck converter, as shown in Fig. 12(a), and Quasi resonant ZCS (resonant inductor is in series with device) switching buck converter, as shown in Fig. 12(b), based on buck topology are presented in Fig. 12. Quasi resonant converters resemble conventional PWM converters. In addition to reduced switching losses, quasi-resonant converters able to integrate non-idealities of switches, diodes, inductors and transformers into converter operation which otherwise generate spikes is a major advantage (Liu and Lee, 1984, 1990). However, quasi-resonant converters no longer able to compensate load and input disturbances through duty ratio modulation thus adopt frequency modulation. Further, non-idealities introduced by resonant components incurs additional voltage drops and thus limits higher voltage gains and power levels. Also, switches are subjected to higher voltage, current stress. A unified approach in analyzing quasi-resonant converters are presented in (Wu et al., 1999). Detailed advantages and drawbacks of quasi-resonant converters are reported in (Liu and Lee, 1984, 1990). Abilities of quasi-resonant converters in comparison to conventional PWM converters are reported in (Schlecht and Casey, 1988). Two major classes of quasi-resonant converters, ZCS-QRC (favors smooth turn off) and ZVS-QRC (favors smooth turn on) at an expense of increased switch current and voltage stress are detailed in (Zhang and Huang, 1991). Also, constant frequency quasi resonant converters are detailed in (Maksimovic and Cuk, 1991; Anderson et al., et al., 1991; Erickson et al., 1989).

Multi resonant converters can integrate merits of ZCS and ZVS Quasi resonant converters by replacing PWM switches of classical dc/dc converters at an expense of increased circuit complexity and component count (Tabisz and Lee, 1989a, 1989b; Nuno et al.,1992). However, switches still suffer from soaring current and voltage stress and variable frequency operation still remain major disadvantage. Operating frequency range is highly vulnerable with PV voltage fluctuations. Constant frequency MRC with clamped switch voltage are presented in (Farrington et al., 1990; Chau et al., 1996).

Compared to QRC and MRC topologies, constant switching frequency active clamped quasi resonant fly back converters are more attractive for solar grid integration applications at lower power levels due to their simplicity. A Basic fly back converter suffers from huge voltage and current impressions on switches, high di/dt turn off on secondary diodes. Solutions such as RCD snubber (Zhang et al., 2010; Wang et al., 2016) clamps voltage stress on switches to lower levels by dissipating leakage energy into snubber resistance. Instead of dissipating, active clamp technique (Yoshida et al., 1992; Jr, 1986; Henze et al., 1988) recycles leakage energy. Further, it magnetizes fly back transformer with bidirectional current to eliminate switching losses at expense of increased conduction losses in transformer. On the other hand, range of soft switching is highly limited which is extended by adding a resonant inductor in series to fly back transformer. Leakage inductor on resonating with switch capacitance eliminate switching losses in power switch, auxiliary switch and secondary diode. In addition, transformer is magnetized with unidirectional current to limit conduction losses in transformer (Watson et al., 1994; Harada and Sakamoto, 1990; Watson et al., 1996). Soft turn off of secondary diode offer significantly reduced noise in secondary and snubber free operation. High voltage gain applications such as solar grid integration expect slow diodes in secondary, thus active clamped fly back converts are of choice in particular. A secondary active-clamped flyback converter

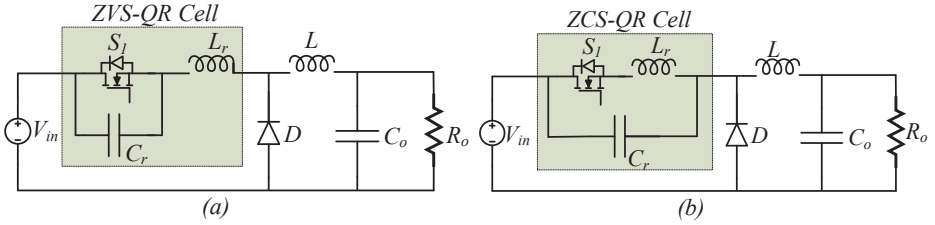

Fig. 12. Converting classical dc/dc converters into quasi-resonant converters. (a) Buck derived ZVS quasi-resonant converter. (b) Buck derived ZCS quai-resonant converter.

(Xue and Zhang, 2018) and auxiliary cell assisted flyback converter (Tarzamni et al., 2017) are also discussed.

Symmetrical and asymmetrical voltage fed full bridge converters augmented with voltage doubler are presented in (Isurin and Cook, 2001; Do, 2012). Such converters are also intended for PV applications as they offer higher voltage gain, grid isolation, clamped switch voltages, constant operating frequency. However, due to voltage fed FEI, input current ripple demands bulky unreliable electrolytic capacitor.

Converters with constant input current, i.e., current fed type, can eliminate requirement of bulky capacitive input filter. Such converters can extend converter reliability in par with PV panel life time. However, current fed converters suffer from switch turn off spike which forces them to adopt FEI with active clamping technique (Dobakhshari et al., 2016, 2017; Zeng et al., 2002; York et al., 2013; Park et al., 2012; Park and Choi, 2012). A current fed transformer assisted auxiliary step-up circuit based non-isolated quasi resonant converter can offer higher voltage gain at expense of increased component count limited at lower power levels (Park et al., 2012). A current fed quasi resonant boost half bridge dc/dc converter can offer high voltage gain at expense of bulky inductive output filter (Zeng et al., 2002). An interleaved version with capacitive output eliminates these demerits (Park and Choi, 2012). Integrated boost quasi-resonant converter with FEI as shown in Fig. 9(c) and leakage inductor as resonant is discussed in (Dobakhshari et al., 2016, 2017). They adopt voltage doubler as RER for higher voltage gain and compact transformer turns ratio. Though (Dobakhshari et al., 2016, 2017; Zeng et al., 2002; York et al., 2013; Park et al., 2012; Park and Choi, 2012) offers compact size, constant input current, fixed frequency operation, a clamping capacitor is mandatory thus compromises the reliability of the converter. Unclamped current fed quasi resonant converters certainly enhance life time of converter in par with PV panel under such conditions. A high efficiency clamp less half bridge current fed multi resonant converter (FEI: Fig. 13(a); resonant tank: Fig. 6(c7)) offers soft transition in switches (Yuan et al., 2010). A clamp-less full bridge counterpart (FEI: Fig. 13(b)), discussed in (Chen et al., 2008), offers high voltage gain and reliability at expense of variable operating frequency. A comparison of a current-fed resonant and quasi-resonant converter topologies has been outlined in Table 2.

Impulse resonant converters, are a special class of quasi resonant converters. This technique has been verified on various FEIs such as push pull (as shown in Fig. 13(c)) (Sree and Rathore, 2015, 2017a; Kim et al., 2014), full bridge (Sree and Rathore, 2017b) (as shown in Fig. 13(b)) and half bridge (Sree and Rathore, 2016) (as shown in Fig. 13(a)). Impulse resonant converters also offer high voltage gain, high reliability at expense of compromised efficiency and variable switching frequency. Conventional time domain analysis for steady state and dynamic modelling are valid for quasi resonant converters. Major drawback of impulse converters is variable frequency operation and higher peak currents.

3.2 HF pulse width modulated (PWM) dc/dc converters

A. Voltage-fed PWM dc/dc converters

Isolated power electronic dc/dc converters can be classified into two categories: (1) single-ended topology and (2) double-ended topology depending upon the core utilization of the transformer. Flyback and forward converters are the two main single-ended topologies. Flyback converter is the most popular single-ended voltage-fed PWM converter for PV system due to its cost effective and single-switch simple configuration. Due to its poor core utilization, Flyback converter is suitable for low power applications such as solar microinverter. Push-pull, half-bridge and full-bridge configurations are three basic double-ended topologies as shown in Fig. 14. The core utilization of double-ended topologies is better, which reduces the volume and weight of the converter offering high power density. The transformer in double-ended topologies can further be optimized over full duty cycle range. Full-bridge topology is modular, scalable and is preferred for higher solar power applications.

Phase-shifted modulation technique is widely adopted for PWM dc/dc conversion in full-bridge topology (Sabate et al., 1990). The energy stored in the leakage inductance of the transformer is utilized to achieve ZVS soft-switching of the semiconductor devices. This technique suffers from the problem of limited soft-switching range. The lagging-leg of the full-bridge converter tends to lose ZVS at light load conditions. The ZVS range can be extended by increasing the leakage inductance of the transformer or by adding an external series inductor (Gautam et al., 2011). However, adding a large series inductance reduces the power transfer capability of the converter due to the effective duty cycle loss of the converter. Additional auxiliary circuits have been proposed to extend the ZVS range , however a considerable amount of power is dissipated in the auxiliary circuits and the circuit is much more complex (Wijeratne and Moschopoulos, 2014; Jain et al., 2002; Wu

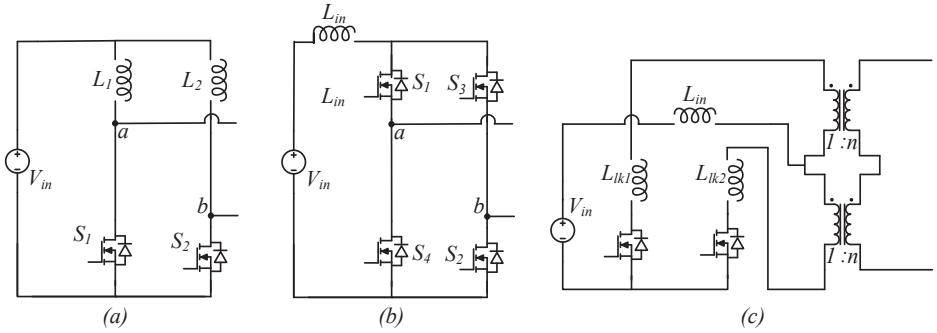

Fig. 13. Clamp less FEI (a) half bridge (b) full bridge (c) push–pull.

Table 2
Comparison of Current-fed Resonant and Quasi resonant converters.

Parameter	LCC-T (Vakacharla and Rathore, 2019c)		LLC-SRC (Vakacharla and Rathore, 2019b)	Quasi resonant (Yang et al., 2002; Dobakhshari et al., 2017; York et al., 2013)
Output power	300 W		300 W	300 W
Output voltage	380 V		380 V	380 V
Input voltage	30 V		30 V	30 V
Frequency of operation	128 kHz		150 kHz	100 kHz
Load compensation	PWM		PWM	PWM
Semiconductor ratings				
Diode	Average current	0.8A	0.8A	0.8A
	Blocking Voltage	380 V	380 V	380 V
	Turn-on	ZVZCS	ZCS	ZCS
	Turn-off	ZVZSC	ZCS	Hard
Main switch	RMS current	14.4A	13.7A	16.3A
	Peak current	26A	23.33A	30.35A
	Peak voltage	110 V	110 V	110 V
	Turn-on	Hard	ZVS	ZVS
	Turn-off	ZCS	Hard	Hard
Auxiliary Switch	RMS	1.47A	3.14A	4.34A
	peak	2.6A	6A	10.77A
	Peak voltage	110 V	110 V	92 V/110 V
	Turn on	Hard	ZVS	ZVS
	Turn off	ZCS	Hard	Hard
Resonant tank				
L_r	9.26uH	4.66uH		2uH
C_s	22nF	291.78nF		NA
C_p	44nF	NA		NA
L_m	NA	37.348uH		NA
Gain offered by tank	1.8	0.9		NA
Transformer				
Currents at full load	8.48A	10.13A		13.1A
Currents at light load	5.4A	1.5A		1.3A
Transformer voltage rating	54 V		54 V	54 V
Transformer VA rating	457.92VA		547.02VA	707.4VA
KW/KVA rating	1.526		1.823	2.358
TUF	65.51%		54.8%	42.4%
Transformer turns ratio	1:2		1:5.5	

et al., 2006).

Voltage-fed PWM converters also suffer from the issue of voltage overshoot and ringing across rectifier diodes, which are caused by the resonance between the transformer leakage inductance and parasitic capacitance of the rectifier diodes. RCD snubber circuit (Mweene et al., 1991) and an active-clamping circuit (Sabate et al., 1991) are often used to suppress the voltage spikes across the diodes. Several energy recovery clamp circuits (ERCCs) have also been proposed to accommodate the issues of the voltage spikes in (Ilic and Maksimovic, 2007; Xinke et al., 2007; Cha et al., 2008). Although such techniques are able to solve the problem, they increase the complexity of the converter and degrade the efficiency.

In addition to the above issues in voltage-fed PWM converters, during the freewheeling intervals, the reflected load current circulates through the primary side, causing additional conduction loss. The rectifier diodes are replaced with active switches in (Cacciato et al., 2010; Hu et al., 2019) to allow additional freedom to achieve wide range of soft-switching and reduced conduction loss. The obvious drawback is the high count of active switches and high cost.

B. Current-fed PWM dc/dc converters

Voltage-fed topologies employ large electrolytic capacitor resulting in large size, high cost and shortened lifetime. These shortcomings are in conflicts with overall requirements of dc/dc converters for PV systems. Compared with the voltage-fed converters, current-fed converters offer the following merits. (1) Lower input current ripple or nearly stiff dc current, which is beneficial to extract maximum power from PV. (2) Lower transformer turns-ratio: Current-fed converters are boost derived converters and have built-in boost function. Therefore current-fed converter results into lower transformer turns ratio, which can simplify the design and reduce losses. (3) No diode ringing and free from duty cycle loss due to purely capacitive output filter. (4) Easier current control ability. The input current can be directly and precisely controlled.

With these merits, current-fed converters have been justified and

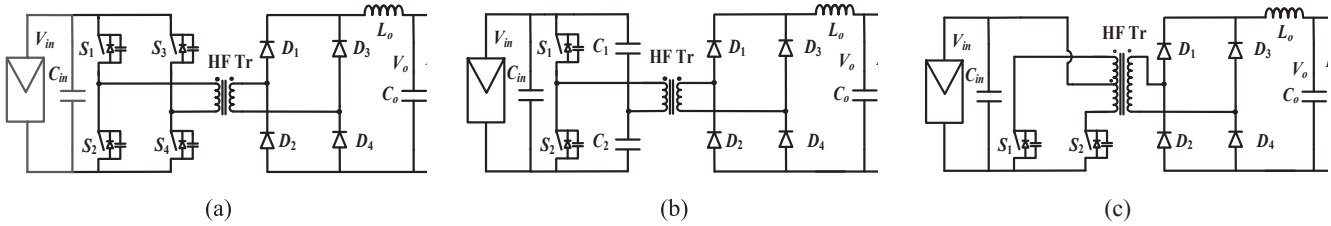

Fig. 14. Voltage-fed HF transformer isolated dc/dc converters. (a) full-bridge converter (b) half-bridge converter (c) push–pull converter.

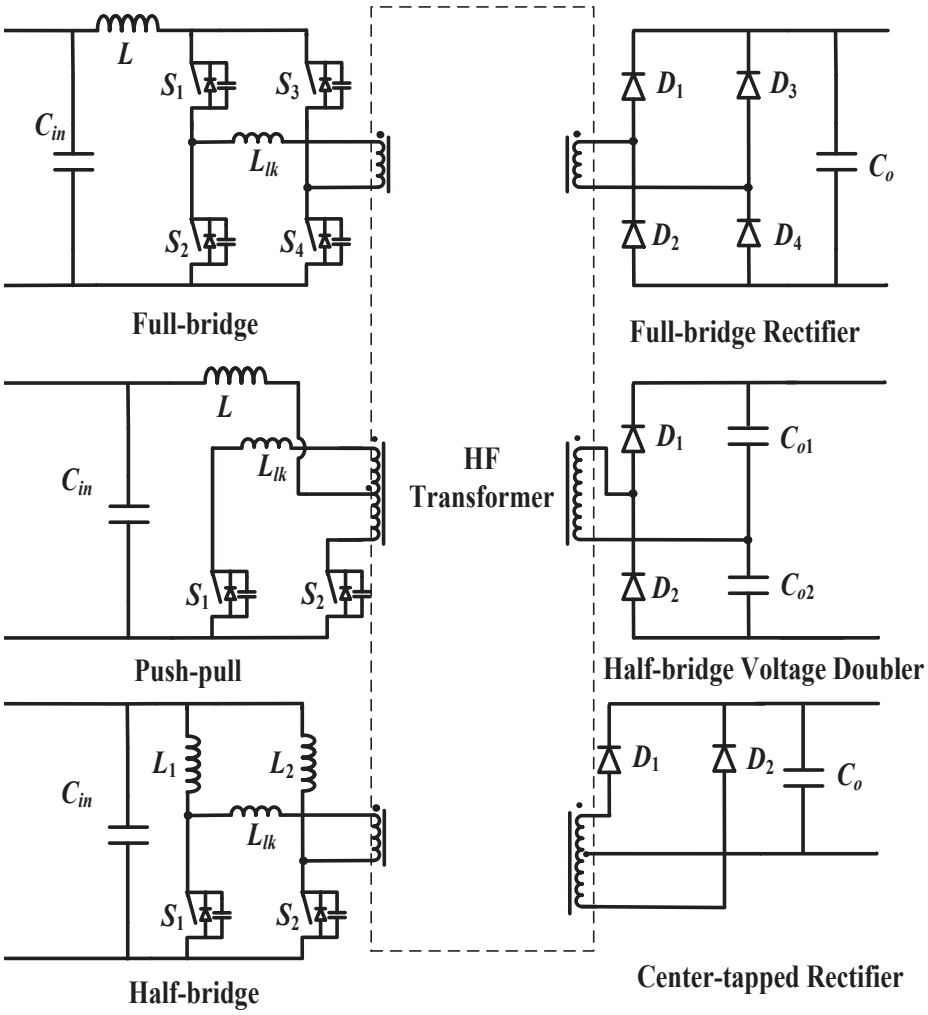

Fig. 15. Typical current-fed PWM dc/dc converter topologies.

demonstrated as a suitable option for PV applications. Different topologies of current-fed PWM dc/dc converters have been researched. As illustrated in Fig. 15, full-bridge, half-bridge, and push–pull topologies have been proposed for the low voltage side inverter stage. For the high voltage side rectifier stage, there exist some popular topologies like full-bridge diodes rectifier, half-bridge voltage doubler, and center-tapped rectifier.

B.1. Traditional current-fed dc/dc converter with snubber or auxiliary circuits

The major drawback of current-fed converter is high voltage spike across device at turn-off owing to the energy stored in the leakage inductance (Bleijs and Gow, 2001; Morten and Andersen, 2010; Jang et al., 2007). Snubbers are generally required to limit the voltage spike to prevent the switching device from a permanent breakdown. Different snubber circuits such as dissipative snubbers, and regenerative snubbers have been proposed as shown in Fig. 16. These snubbers are employed to accommodate the whole boost inductor current until the HF transformer current is fully built up to the level of the boost inductor current. The LC snubber stores the surge energy in the capacitor during device turn-off. Once the switch is turned on, the capacitor is reset and energy stored in the inductor is fed back to the input instead of being dissipated. However, the conventional LC snubber has several problems like complex structure; difficult optimal design, and do not assist in soft-switching.

In (Wu et al., 2010), an auxiliary flyback snubber including a capacitor, a diode and a flyback converter was introduced to recycle the absorbed energy. The flyback snubber alleviates the voltage spike and transfers the trapped energy to the load. The circuit operates with hard switching.

Another approach is to apply ZCS to divert the current away from the switches before turning them off. In (Averberg et al., 2008), external auxiliary circuits are utilized to achieve ZCS and reduce the circulating current for current-fed full-bridge topology. In (Leung et al., 2007), the transformer leakage inductance and device output capacitance are used to create a quasi-resonant path to facilitate ZCS. The shortcoming is that four extra diodes are connected in series with the main switches to reduce the circulating loss. This brings more conduction losses and increases the cost and circuit footprints. For the topology proposed in (Wang et al., 2009), an external circuit consisting of two uni-directional switches and a resonant capacitor is employed to obtain ZCS turn-on/off of the switches. The ringing due to the interaction of the transformer leakage inductance and switch capacitance is major limitation of this technique. Higher voltage rating devices or dissipative snubbers are needed. In (Mousavi et al., 2012), an external boost converter is added to provide a path for the boost inductor current and send the trapped energy to the load. A small inductor is needed to achieve ZCS turn-on /off. Although the trapped energy can be recycled, the auxiliary circuits still contribute to a significant amount of loss. The higher cost and circuit complexity are two major concerns.

Similar external snubber or auxiliary circuits can be adopted for

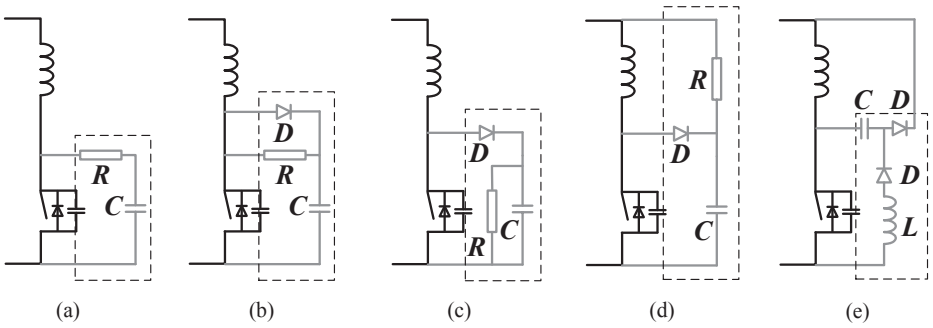

Fig. 16. Snubbers for suppressing the voltage spike: (a) Dissipative RC snubber, (b)(c)(d) Dissipative RCD snubber, (e) Non-dissipative energy recovery LC snubber.

other topologies too. But they add to the cost and volume and not scalable for higher power application owing to loss of modularity. In addition, boost capacity is compromised and it requires additional secondary turns in transformer.

B.2. Active clamped current-fed dc/dc converters

A simple way to suppress the voltage spike inherited in current-fed converter is to utilize power semiconductor devices and a large HF film capacitor to provide an additional commutation path. It allows the current flowing through the leakage inductance to rise to the input inductor current in a controllable manner. The voltage spike can be considered to be clamped by the HF film capacitor. Thus this is called active clamp technique. The energy stored in the leakage inductor can be recycled, thus solving the energy loss problem. With a proper parametric design, ZVS of primary switches can be achieved.

Active clamp has been implemented in many fundamental topologies, such as full-bridge current-fed topology (Liu et al., 2019) as shown in Fig. 17, several examples of typical current-fed L-L type half-bridge topologies as displayed in Fig. 15 (Jang et al., 2007; Rathore et al., 2012; Hu et al., 2015), push–pull topologies (Wu et al., 2008; Kwon et al., 2009a,b). The active clamp technique can be applied to three basic double-ended topologies. All of them can achieve ZVS soft-switching of all switches and have higher efficiency compared to dissipative/passive snubbers. However, they all suffer from the demerits of additional floating devices, driver, and large HF capacitor adding to volume. Compared with active clamped full-bridge topology, L-L type half-bridge and push–pull topologies have less number of active switches and potential lower input current ripple with interleaving effect. The utilization of HF transformer of push–pull topologies is poor. The L-L type active-clamped converter can achieve higher boost ratio on account of equivalent dual boost converters on primary side.

Peng et al., proposed a novel type of current-fed dc/dc converter with a single boost half-bridge as shown in Fig. 18 (Cao et al., 2012). This topology is a boost type circuit and minimizes the devices count for the same power rating compared to full-bridge topology, which allows a compact packaging. Each switch and corresponding capacitor will serve as the active clamp for the complementary one. Practically, the ZVS soft-switching can't be maintained through full range of load. Another

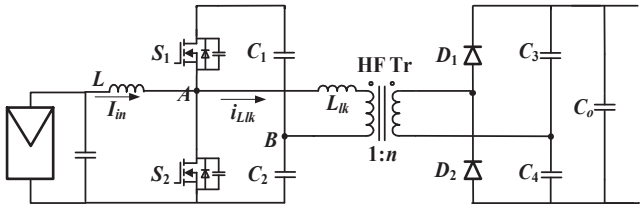

Fig. 18. Current-fed dual half bridge dc/dc converter.

drawback of half-bridge topology is the requirement of split capacitors which have to deal with the full load current.

Similar active clamp techniques have been reported for three-phase current-fed topologies (Hu et al., 2014). Three-phase converter not only inherits the advantages of aforementioned single-phase current-fed converters but also increases the power transfer capability switches with the same voltage and current rating compared to single-phase one. In addition, reduced RMS current per phase and low conduction loss and smaller size of passive components are achieved for the same power compared to the single-phase converter.

B.3. Natural clamped current-fed dc/dc converters

Naturally-clamping for current-fed converters was introduced in (Prasanna et al., 2013) and proposed a great contribution to develop a new family of current-fed converters and solve the traditional issue of device turn-off voltage spike without additional snubber. The main principle of secondary-modulation-based naturally clamping technique is to utilize the reflected output voltage across the primary winding of the HF transformer. The reflected output voltage diverts the input boost inductor current from one switch (or switch pair) to the other switch (or switch pair) through the HF transformer. A minor circulating current allows body diode conduction to ensure ZCS and natural turn-off. Low voltage side switches are naturally voltage clamped by reflected output voltage and achieve ZCS turn-off and nearly ZVS turn-on, while the high voltage side switches realize ZVS turn-on.

Two types of secondary-modulation have been implemented over current-fed half bridge topology and full bridge topology as shown in Figs. 19 and 20 (Prasanna and Rathore, 2013; Xuewei and Rathore,

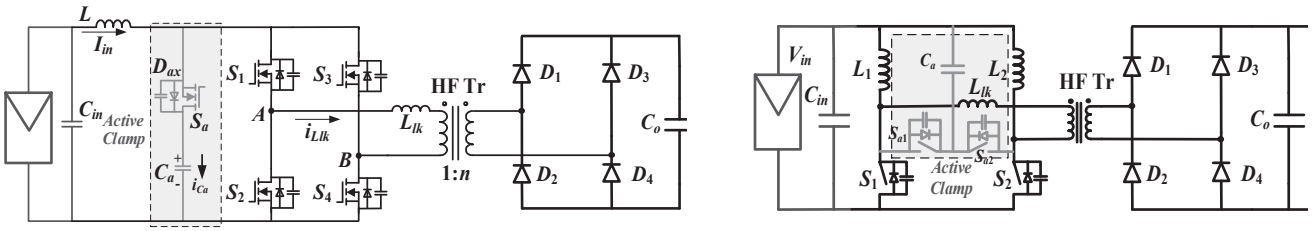

Fig. 17. (a) Full-bridge and (b) half-bridge current-fed converter with simplest active clamp.

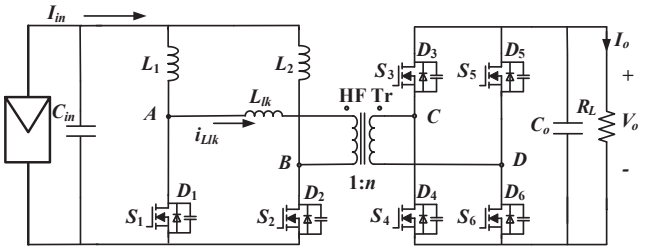

Fig. 19. Natural clamped current-fed half-bridge dc/dc converter.

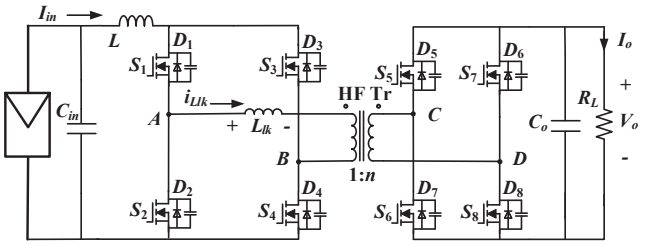

Fig. 20. Natural clamped current-fed full-bridge dc/dc converter.

2014; Bal et al., 2018). The key operating waveforms of these two secondary-modulation techniques have been displayed in Fig. 21. Both of them can achieve natural voltage clamping while for (Prasanna and Rathore, 2013) the current flowing through HF transformer is discontinuous unlike (Xuewei and Rathore, 2014). Thus the control method proposed in (Prasanna and Rathore, 2013) suffer from the oscillation due to the resonance between the leakage inductance of HF transformer and device capacitances when current in the transformer reaches zero.

For both of these two techniques (Prasanna and Rathore, 2013; Xuewei and Rathore, 2014), at light loads conditions, the peak current through the leakage inductance of HF transformer and the low voltage side switches is much higher than the input current. As a result, the performance of the converter is reduced at light loads. (Bal et al., 2018) proposes dual phase shift (DPS) modulation implemented over the same topology. In addition to φ, the phase difference α_s between the diagonal switches on high voltage side is also controlled. With this modified modulation strategy, the value of aforementioned peak current is greatly reduced and thus the performance of the converter is improved at light load conditions. However, such converters tend to be expensive for unidirectional applications due to increased high side switches and driver circuits (Pan et al., 2020).

B.4. Impulse commuted current-fed dc/dc converters

Impulse commutation utilizes transformer leakage inductance and interturn winding capacitance as the resonance tank, which allows the device voltage to rise gradually and therefore solve the issue of device turn-off voltage spike without increasing complexity and degrading performance of converters. It should be noted that it is not a resonant converter. Owing to boost nature and modulation, the resonance happens only for a short period of time depending upon the overlap time. During this resonance impulse, the circulating current flows through the anti-parallel body diode of the devices causing ZCS device turn-off and also gives rise to peak current. Therefore, the design of the impulse circuit should be to limit the body diode conduction time and hence, the peak/circulating current to limit the conduction losses. Since, this is not a resonant converter, the peak current is limited.

Impulse commutation technique can be applied to three basic double-ended topologies L-L type half-bridge, push–pull, and full-bridge (Sree and Rathore, 2015, 2016) as shown in Fig. 22. Reduced peak and circulating currents compared to resonant converters with identical LC tank are achieved for impulse commutated current-fed converter. Therefore, the efficiency of impulse commutated current-fed dc/dc converter can be maximized compared to resonant converters. The gain is immune to the load, meaning that with load current variation, the voltage is regulated with no frequency or light frequency variation. Frequency modulation is employed to regulate load voltage with variation in source voltage. The demerits of impulse commutated current-fed converter can be summarized as: (1) Frequency variation to regulate load voltage with source variability, (2) Increased diode conduction time with increase in input voltage, (3) optimum design of LC tank to limit frequency variation to limit switching losses and simplify filter design.

4. Low frequency multilevel converters

To integrate the large scale photovoltaic power plants (MW level), high power converters operating at medium voltage or high voltage conducting high current are needed. For the past two decades, the trend has been in replacing two-level topologies by on multilevel topologies in high-power applications such as flexible AC transmission systems (FACTs), static synchronous compensator (STATCOM), high voltage DC

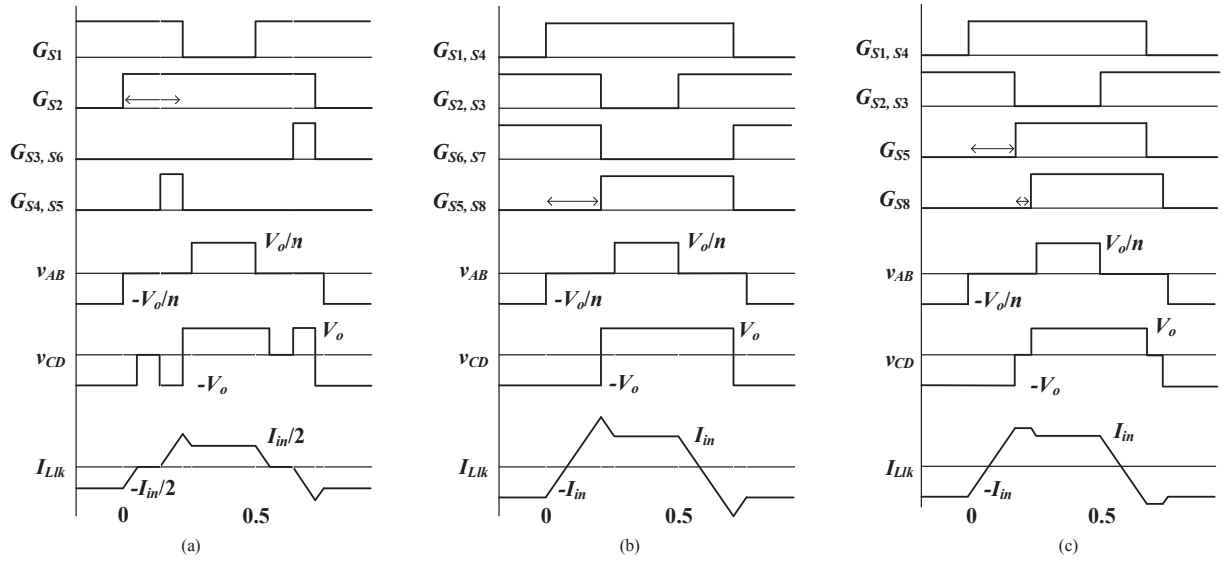

Fig. 21. Key operating waveforms of three types of secondary-modulation-based naturally clamping techniques.

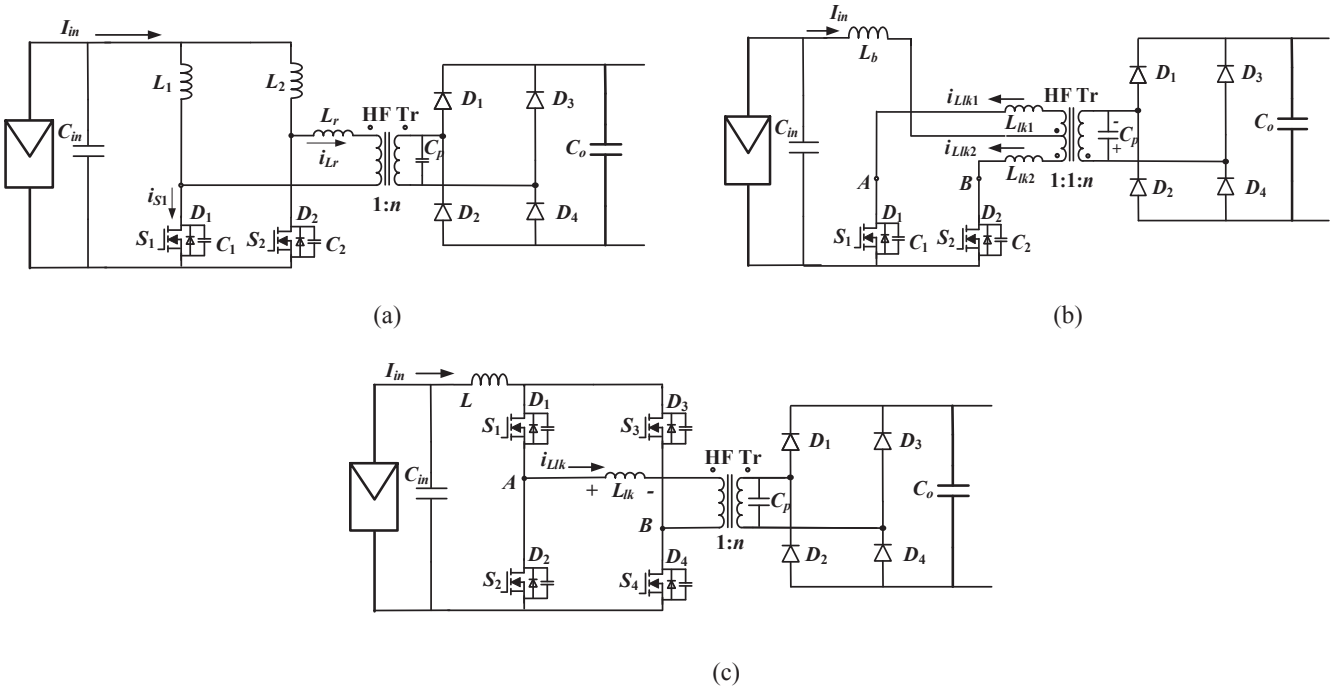

Fig. 22. Impulse commuted current-fed (a) half-bridge, (b) push–pull and (c) full-bridge dc/dc converter.

(HVDC), medium voltage DC (MVDC), ship propulsion, electric vehicle, more electric aircraft, solar PV energy conversion and wind energy conversion system (Kouro et al., 2010). Numerous multilevel inverters have been proposed as well as available in the market for solar PV conversion systems. Some of these topologies along with their merits and limitations are discussed next.

Introduction of multilevel converters (MLC) has emerged in the late 1960s (McMurray, 1971). The aim of the power converter stage at solar PV system is to convert the available dc power into sinusoidal ac power. The converter output waveform from MLC replicates sinusoidal waveform while comparing with the classical two-level PWM waveform. Some of the notable advantages of MLC are high-quality waveforms, reduced filter sizes, transformer-less topology, low dv/dt stress, high power handling capability using low voltage semiconductor devices, etc. The MLC can also be classified as current-fed MLC and voltage-fed MLC. The converters that bring multilevel in the current waveform are referred as current-fed MLCs and the converters that bring multilevel in the voltage waveform are referred as voltage-fed MLCs. The voltage-fed MLCs have extensively been researched for the past few decades (Carrasco et al., 2006) whereas the current-fed MLCs are in their initial research stage.

4.1. Voltage-fed MLC

Voltage-fed MLCs have been researched extensively for the past few decades (Carrasco et al., 2006). The multilevel in the voltage is achieved by using multiple capacitors in case of single sourced MLC topology. Each level is contributed by one of these capacitors' voltage. The desired output level is achieved by turning-on or turning-off the semiconductor devices connected across the respective capacitors. For developing a multilevel topology, these capacitors can be connected in different ways to classify voltage-fed multilevel converters as neutral point clamped (NPC) MLCs (Nabae et al., 1981), flying capacitor (FC) MLCs, cascaded H-bridge (CHB) MLCs, hexagram MLCs and hybrid MLCs (Kouro et al., 2010; Yin et al., 2019). Among these topologies NPC, FC and CHB are well established and treated as classical voltage-fed MLC topologies. There are various voltage fed MLC topologies are recently developed (Rodriguez et al., 2007) but in this section only the MLC topologies that are developed for solar PV application and how these topologies mitigate the issues when used for solar PV applications are discussed.

A. Neutral point clamped (NPC) topology

In NPC, (L-1) number of capacitors are connected in series to obtain *L*-level voltage waveform at the converter output (Wang et al., 2017). The topology is shown in Fig. 23 is a three-level NPC topology. Each capacitor is equally charged to a voltage value of V_{dc}/L using 6(L-1) number of semiconductor devices. Recently, the NPC topology has been modified into different configurations such as active-NPC to replace the diodes with the active semiconductor devices to provide full control on the neutral point (Wang et al., 2017) and advanced T-type NPC (AT-NPC) to enable low conduction loss of the converter (Fujii et al., 2013). Fuji Electric has manufactured a highly efficient high power (1 MW) solar inverter using the AT-NPC. The charging of series capacitors in NPC converter can be utilized to handle the partial shading problem. In case of large-scale PV plants, the partial shades on some photovoltaic modules lead to reduced power generation from its potential maximum power. This has been overcome by connecting each PV string or PV module to one of the capacitors at the NPC input (Busquets-Monge et al., 2008). By doing so, the capacitor voltages are independently controlled to obtain the maximum power from the respective PV strings/modules connected to the capacitor. This modified arrangement with the independent voltage control technique helps to achieve 30%

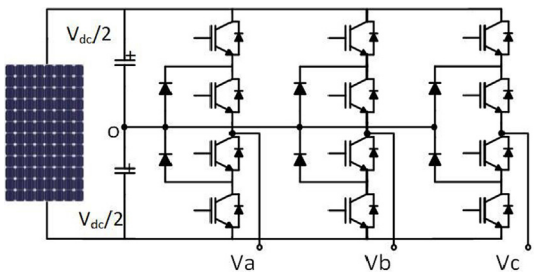

Fig. 23. Neutral point clamped MLC.

more power extracted as that of the conventional NPC.

Another modified NPC (Sahoo and Keerthipati, 2017) is a voltage boost NPC. It combines LC-switching boost stage with the NPC topology. The modified voltage boost NPC helps to achieve desired multilevel waveform with a single converter structure and it avoids a need for additional dc/dc converter for boosting low voltage from PV modules.

The NPC topology can be extended to any number of voltage levels. However, with the increased number of voltage levels, the number of semiconductor devices will also increase that reduces reliability. In Sivakumar (2015), a fault tolerant multilevel NPC has been proposed in which the modulation and control technique is implemented to operate the converter during faulty conditions. The converter is operated to transfer the PV power without any interruption even in a faulty condition with the help of an additional multi-tapped transformer. However, this operational benefit comes with the cost of losing one or more levels from the multilevel converter.

B. Cascaded MLC topology

Another classical topology that is widely researched for solar PV application is cascaded H-Bridge topology. The topology needs multiple dc sources to obtain the multilevel waveform. Large scale PV plants are built with multiple PV modules (as multiple sources) and therefore, the CHB topology is the best suited voltage-fed MLC for PV application. CHB topology is made of series connection of H-bridge outputs connected to PV modules. The input to the H-Bridge is either PV modules/ PV strings as shown in Fig. 24. Compared to the NPC topology, the CHB is simple to build due to its modular structure. However, the number of sources needed in case of CHB is $3L$ where L is the number of levels in CHB MLC. Whereas in NPC, a single source is sufficient to produce L levels. For CHB MLC the number of H-bridges decides the number of levels at the output (Villanueva et al., 2009). For n_{HB} count of H-bridges there is $L = 2n + 2$ number of multi-levels are possible. The modularity nature of CHB MLC makes it easy to extend it to higher voltage levels.

Three-phase power generated from the NPC topology is balanced since the same set of sources are utilized to produce the three-phase power. However, with the CHB, the PV modules are connected individually for each phase and thus it brings unequal power generation between the phases if the solar irradiance and module temperatures are unequal (Sharma and Das, 2019; Amaral et al., 2018). The difference in the solar irradiance is unavoidable in case of large-scale PV power plants. A zero-sequence injection-based controller is designed in (Yu et al., 2016) for CHB to integrate balanced three phase power to grid even when there is unequal solar irradiance between the panels in the phases. Another way of handling the unbalanced power between phases is to replace the star connected three-phase in CHB to delta connected three phases (Yu et al., 2017). This modification in the cascading structure will circulate zero sequence current due to the unbalanced power within the delta connection. To withstand the circulating zero sequence current using delta connection, the semiconductor devices in CHB has to be overrated.

To handle basic faults in the converter such as short circuit fault, open circuit fault, or double short circuit fault, an external/ internal bypass strategy along with three-phase power balance controller is proposed in (Yu et al., 2015). It provides uninterrupted power to the grid even when there is a fault in the converter devices. In (Stonier and Lehman, 2018), an artificial neural network-based method has been proposed to detect the 20 types of faults (includes solar PV faults and inverter faults) that can occur during the operation of the converter. In addition, an auxiliary inverter is connected with the CHB to mitigate the identified faults (Stonier and Lehman, 2018).

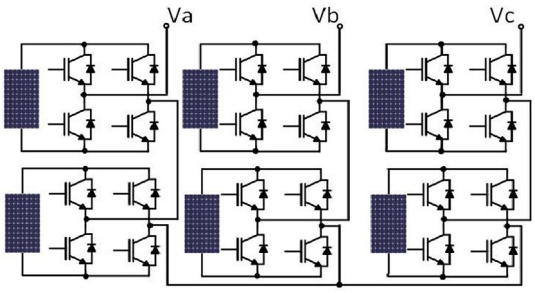

Fig. 24. Cascaded H-Bridge MLC.

Another challenge with respect to CHB topology is tracking the maximum power of the PV modules. The H-bridge outputs are serially connected in CHB. If one of the panels is receiving less radiance then it will bring down the other PV modules of the phase leg from their maximum power point. Hence, the H-bridges need to be programmed with maximum power tracking controller to extract maximum possible power. A mixed staircase PWM technique with sorting algorithm has been utilized in (Coppola et al., 2016) to control the serially connected H-bridges and maximum power of each PV modules are tracked independently using this technique.

A modified cascaded version of this topology is proposed in (Achanta et al., 2019) where H-bridges are replaced with three-phase bridge circuits resulting in conversion of dc power from each PV module in cascaded MLC directly to three-phase power. It avoids the power imbalance issue caused by shading on PV modules. Another advantage is that it eliminates the need for low-frequency transformer for MVAC grid integration (Achanta et al., 2019).

C. Modular multilevel converters (MMC)

An emerging MLC topology named Modular Multilevel converter (MMC) is becoming an interesting research topic in the multilevel topologies and widely applied in case of single dc source applications. Recently, the MMC topologies have also been researched for solar PV applications (Rong et al.,2017; Islam et al., 2017; Mei et al., 2013; Nademi et al., 2016; Lizana et al., 2016). The MMC topology is shown in Fig. 25. It contains three upper and three lower arms with two arm inductors between upper and lower arm. Each arm consists of n number of sub-modules. A submodule can be constructed with either half-bridge with capacitor (Mei et al., 2013; Nademi et al., 2016) or full-bridge with capacitor (Lizana et al., 2016). The usage of MMC is not that popular as NPC and CHB because of circulating current and capacitor voltage balancing problem. It restricts the solar inverter efficiency and the uncontrolled circulating current can make the system unstable (Ilves et al., 2012). The circulating current magnitude depends on the number of sub-modules used in the arms. As the large scale solar PV system handles high power, the MMC needs to utilize higher number of sub-modules per arm. Therefore, the circulating current is inexorable for solar PV plant. Though the arm inductors are placed in each phase of MMC to limit the magnitude of circulating current, they might not be sufficient enough to completely control the circulating current. To solve this issue, a selective virtual loop mapping technique has been proposed in (Mei et al., 2013). The technique utilizes a virtual sub-module to balance the capacitor voltages so that the circulating current is reduced. In (Lizana et al., 2016), the capacitor voltage balancing is achieved by using voltage transformation method in which the four energy components are controlled. In (Nademi et al., 2016), the arm inductors are replaced by an open-end transformer to reduce the voltage rating of the devices by half and to reduce the number of cells by half for the same voltage multilevel output.

Another point to be noted in single sourced MMC for solar PV is that all the PV modules/strings are connected as an input to the converter. This causes the PV power conversion operating point away from the maximum power point. To enable maximum power tracking for each PV string, a modified version of MMC is developed in (Rong et al., 2017; Islam et al., 2017). In this configuration, the capacitors in sub-modules are replaced with PV module and capacitor. This modification helps to

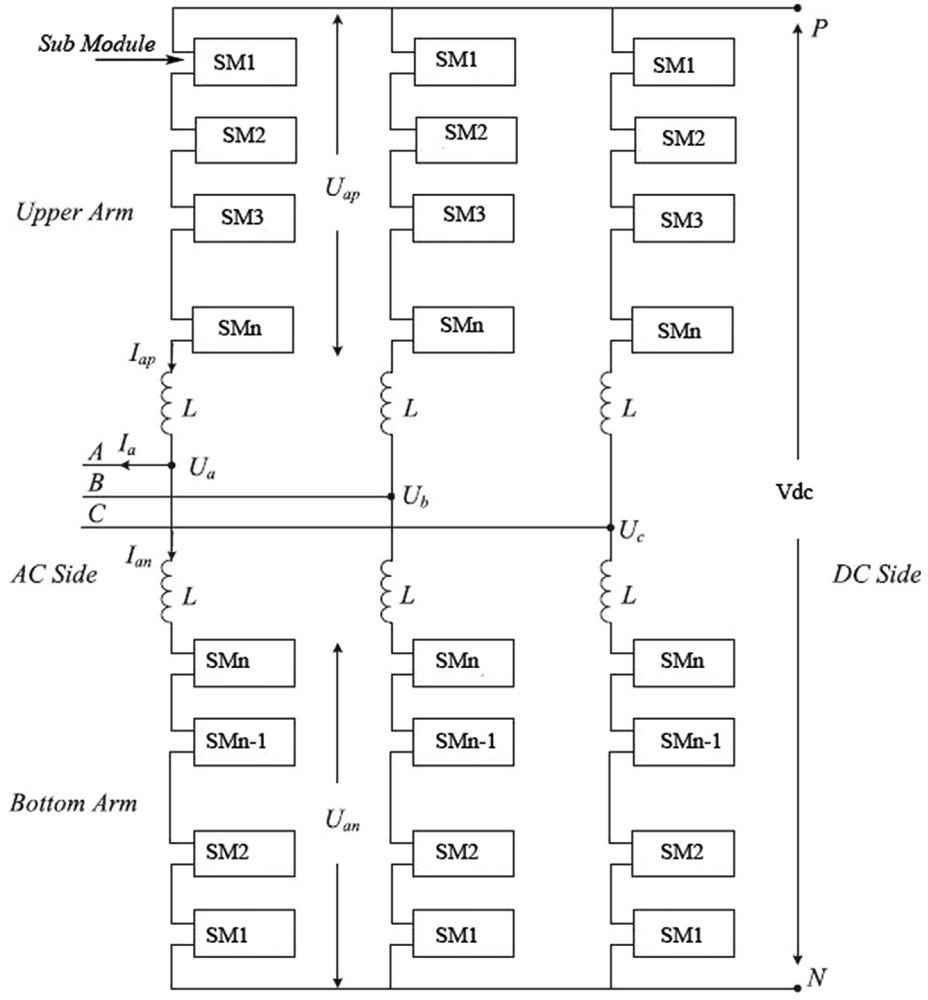

Fig. 25. Modular MLC.

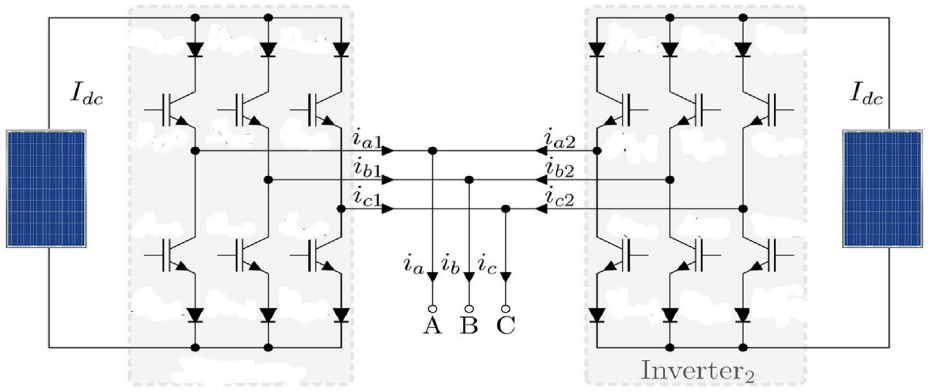

Fig. 26. Current-fed paralleled H-Bridge MLC.

have individual MPPT controller for each PV module. The capacitor connected in parallel with the PV module in the modified MMC will help in reducing the losses due to partial shading by regulating the capacitor voltages (Rong et al., 2017).

4.2. Current fed MLC

Based on the principle of duality between voltage and current sources, several current-fed MLCs analogous to voltage-fed MLCs have been identified. Current-fed MLCs offer several advantages such as high power conversion capability, transformer-less operation, short circuit protection, a longer lifetime as the storage elements are inductors and excellent quality of output current waveforms. The current source nature of the current-fed MLCs enables them as suitable MLC for solar power application. The dc link voltage at the solar PV installation is limited to 1500 V due to the insulation requirement for PV modules (Serban, et al., 2015). Therefore, in order to increase the power handling capability of the converter the only possible way is to increase the current capacity. One of the basic advantages of the MLC topologies is the reduced device current rating. In the case of voltage-fed MLC, the

voltage rating of the devices is reduced; however, the current rating is still the maximum converter handling current. Hence with the dc bus voltage limitation, another way to achieve MW power converter is to utilize current-fed MLCs. The current rating of the devices is reduced to $2/(L-1)$ times by using L-level current-fed MLC (Gnanasambandam et al., 2017). The CHB topology is found to be promising among other voltage-fed MLC topologies. The dual of the CHB in current-fed MLC is paralleled H-bridge converter. The topology of the paralleled H-bridge MLC is shown in Fig. 26. It could be observed that the paralleled H-bridge MLC topology needs independent current sources (Guedouani et al., 2011; Dash and Kazerani, 2011). The parallel H-bridge MLC is a suitable candidate for the solar PV application as multiple dc source can be obtained by connecting to different sets of PV strings (Dash and Kazerani, 2011, 2012; Vekhande et al., 2015). The dc links for the inverter obtained by either connecting the PV module directly or PV module with a front-end dc/dc converter. The dc currents from different PV modules may not be the same due to partial shading and dissimilarities between the PV modules. Under such variations, the MLC output current will contain lower order harmonics. To handle unequal currents, a closed loop controller with space vector modulation (SVM) strategy is needed in order to keep output current within allowable harmonic and THD standards (Vekhande et al., 2015). Another notable issue with this topology is the resonance between the inductor and the filter capacitor, which will introduce the lower order harmonics in the output current. The resonant issue has been overcome in (Zheng et al., 2011), by designing virtual resistor based active-damper in the controller design. The dynamic performance of the converter is decided by the filter size. The filter size will be large if the converters are operated at low switching frequency (< kHz). However, for high power application, the high switching frequency operation increases the switching losses and needs for additional cooling requirement. A novel modulation technique has been proposed (Gnana Samdandam et al., 2019) to achieve reduced filter size by limiting the lower order harmonics as well as achieved better dynamic performance by utilizing the advantages of SVM scheme.

To summarize, at low or moderate power levels, HF power converters are used to accomplish compact, light weight and low cost system. The switching frequency may vary from 20 kHz (medium power) to 1 MHz (low power) based on the specifications. However, high-switching frequency operation of the semiconductor devices results in higher switching losses, thus limiting the power conversion efficiency. Therefore, soft-switching of the semiconductor is implemented to reduce the switching losses, thus realizing high efficiency. The soft-switching can be implemented using PWM techniques or resonant tank. Resonant tank suffers from the demerits of the complex variable switching frequency control and circulating through the components demanding overrated components. Also, optimizing the tank kVA rating or the resonant tank parameters is a challenge to optimize the efficiency and the volume. PWM techniques offer simple control but limited soft-switching range. If the source is variable like solar, then soft-switching range in PWM converters and switching frequency range in resonant converters, become a challenge. Voltage-fed converters suffer from high peak currents if a capacitive filter is used and suffer from duty cycle loss, voltage ringing and snubber requirements if inductive filter is used. On the contrary, current-fed converters offer voltage gain, short circuit protection, current limiting feature, and free from the problems of the duty cycle loss and voltage ringing. However, current-fed converters suffer from the hard device commutation resulting in high voltage spike across the devices at their turn-off. Therefore, auxiliary snubber or clamping circuit is usually required for current-fed converters. For power conditioning a higher power, owing to the unavailability of the higher blocking voltage semiconductor devices, multilevel converters are used. For better device utilization, limit the switching losses, and to limit the cooling requirements, device switching frequency is usually limited to < 1 kHz and currently between 50 Hz and 500 Hz based on the power level. Multilevel converters suffer from the large number of capacitors and device requirements but reduced filtering and cooling requirements and therefore, used for high power generation.

5. Conclusion

This paper is on the enabling technology 'Power Electronics' that is mandatory between source (solar) and the load as the power conditioner. It is an essential requirement to match the specifications of the source and the load as well as to manage the power and energy flow between them subject to the atmospheric conditions. MPPT is also implemented using a switching device (that is power electronics). This paper is an state-of-the-art paper reporting the advances on the MPPT as well as on the power conditioning topologies. This state-of-the-art review paper help to have a quick literature survey and gather information on the advancements of MPPT techniques and solar power converters in a confined manner. In this review article, a comprehensive review and comparison of solar MPPT techniques have been reported. Several high-frequency PWM and resonant dc/dc converter topologies have been reported. These topologies can either be used for MPPT or front-end dc/dc conversion for boosting the solar voltage to meet the load voltage level. Both, the voltage-fed and current-fed PWM and resonant dc/dc converters have been discussed with more emphasis on current-fed converters for solar applications. Soft-switching operation pf these topologies has been discussed to maintain the high efficiency at high switching frequency of the semiconductor devices. Such power converters are good up to medium power applications. For higher power solar generation, multilevel converters have been reported. Various popular voltage-fed MMC topologies and their comparison has been discussed. At last, current-fed multilevel converter is discussed as a new interesting topic of research for solar generation application. In a grid connected system, inverter should comply with IEEE1547, IEC61727, etc., standards to ensure safe integration with grid and eliminate issues like power quality, detection of islanding operation, reduced common mode currents, restricted injection of dc currents into grid to avoid saturation of distribution transformer. Also inverter should adopt decoupling techniques in order to combat second order harmonic power component.

Declaration of Competing Interest

The authors declare that they have no known competing financial interests or personal relationships that could have appeared to influence the work reported in this paper.

References

Achanta, P.K., Johnson, B.B., Seo, G., Maksimovic, D., 2019. A multilevel dc to three-phase ac architecture for photovoltaic power plants. IEEE Trans. Energy Convers. 34 (1), 181–190.

Aganah, K.A., Leedy, A.W., 2011, March. A constant voltage maximum power point tracking method for solar powered systems. In: 2011 IEEE 43rd Southeastern Symposium on System Theory (pp. 125-130). IEEE.

Agrawal, J.P., Kim, S.H., Kim, Lee, C.Q., 1989. Capacitor voltage clamped series resonant power supply with improved cross regulation. In: Conference Record of the IEEE Industry Applications Society Annual Meeting (pp. 1141–1146).

Ahmed, J., Salam, Z., 2016. A modified P&O maximum power point tracking method with reduced steady-state oscillation and improved tracking efficiency. IEEE Trans. Sustainable Energy 7 (4), 1506–1515.

Ahmed, J., Salam, Z., 2018. An enhanced adaptive P&O MPPT for fast and efficient tracking under varying environmental conditions. IEEE Trans. Sustainable Energy 9 (3), 1487–1496.

Al-Soeidat, M., Lu, D.D.C., Zhu, J., 2018. An Analog BJT-Tuned Maximum Power Point Tracking Technique for PV Systems. IEEE Trans. Circuits Syst. II Express Briefs 66 (4), 637–641.

Amaral, F.V., Parreiras, T.M., Lobato, G.C., Machado, A.A.P., Pires, I.A., de Jesus Cardoso Filho, B., 2018. Operation of a Grid-Tied Cascaded Multilevel Converter Based on a Forward Solid-State Transformer Under Unbalanced PV Power Generation. IEEE Trans. Ind. Appl. 54 (5), 5493–5503.

Anderson, S.W., Erickson, R.W., Martin, R.A., 1991. Jan. An improved automotive power distribution system using nonlinear resonant switch converters. IEEE Trans. Power

Electron. 6 (1), 48–54.
Averberg, A., Meyer, K.R., Mertens, A., 2008. Current-fed full bridge converter for fuel cell systems. In: Proc. IEEE Power Electronics Specialists Conference (PESC) (pp. 866–872).
Bal, S., Yelaverthi, D.B., Rathore, A.K., Srinivasan, D., 2018. Improved Modulation Strategy Using Dual Phase Shift Modulation for Active Commutated Current-Fed Dual Active Bridge. IEEE Trans. Power Electron. 33 (9), 7359–7375.
Barbi, I., Gules, R., 2003. Isolated DC-DC converters with high-output voltage for TWTA telecommunication satellite applications. IEEE Trans. Power Electron. 18 (4), 975–984.
Bharath, K.R., Suresh, E., 2017. Design and implementation of improved fractional open circuit voltage based maximum power point tracking algorithm for photovoltaic applications. Int. J. Renew. Energy Res. (IJRER) 7 (3), 1108–1113.
Bhat, A.K.S., Swamy, M.M., 1989. Analysis of parallel resonant converter operating above resonance. IEEE Trans. Aerosp. Electron. Syst. 25 (4), 449–458.
Bhat, A.K.S., 1990. Analysis and design of LCL-type series resonant converter. In: 12th International Conference on Telecommunications Energy, pp. 172–178.
Bhat, A.K.S., May 1991. Analysis and design of a series-parallel resonant converter with capacitive output filter. IEEE Trans. Ind. Appl. 27 (3), 523–530.
Bhat, A.K.S., 1992. Fixed-frequency PWM series-parallel resonant converter. IEEE Trans. Ind. Appl. 28 (5), 1002–1009.
Bhat, A.K.S., 1995a. A fixed frequency LCL-Type series resonant converter. IEEE Trans. Aerosp. Electron. Syst. 31 (1), 125–137.
Bhat, A.K.S., 1995b. A fixed-frequency modified series-resonant converter: analysis, design, and experimental results. IEEE Trans. Power Electron. 10 (6), 766–775.
Bhat, A.K.S., 1997. Analysis and design of a fixed-frequency LCL-type series-resonant converter with capacitive output filter. IEE Proc.-Circuits, Devices Syst. 144 (2), 97–103.
Bhat, A.K.S., Dewan, S.B., 1987. Analysis and Design of a High-Frequency Resonant Converter Using LCC-Type Commutation. IEEE Trans. Power Electron. 2 (4), 291–301.
Biela, J., Badstuebner, U., Kolar, J.W., 2009. Design of a 5-kW, 1-U, 10-kW/dm$^\hbox3$ Resonant DC–DC Converter for Telecom Applications. IEEE Trans. Power Electron. 24 (7), 1701–1710.
Blanes, J.M., Garrigos, A., Carrasco, J.A., Ejea-Martí, J., Sanchis-Kilders, E., 2011. High-Efficiency Regulation Method for a Zero-Current and Zero-Voltage Current-Fed Push-Pull Converter. IEEE Trans. Power Electron. 26 (2), 444–452.
Bleijs, J.A.M., Gow, A., 2001. Fast maximum power point control of current-fed DC-DC converter for photovoltaic arrays. Electron. Lett. 37 (1), 5–6.
Boonyaroonate, I., Mori, S., 2002. A new ZVCS resonant push-pull DC/DC converter topology. In: APEC. Seventeenth Annual IEEE Applied Power Electronics Conference and Exposition (pp. 1097–1100). IEEE.
Borage, M., Tiwari, S., Kotaiah, S., 2005. Analysis and design of an LCL-T resonant converter as a constant-current power supply. IEEE Trans. Ind. Electron. 52 (6), 1547–1554.
Borage, M., Tiwari, S., Kotaiah, S., 2007. LCL-T Resonant Converter With Clamp Diodes: A Novel Constant-Current Power Supply With Inherent Constant-Voltage Limit. IEEE Trans. Ind. Electron. 54 (2), 741–746.
Bucher, A. and Duerbaum, T., 2010. Extended first harmonic approximation in case of LLCC converters with capacitive output filter. In: Melecon 2010 - 2010 15th IEEE Mediterranean Electrotechnical Conference (pp. 1303–1308). IEEE.
Busquets-Monge, S., Rocabert, J., Rodriguez, P., Alepuz, S., Bordonau, J., 2008. Multilevel Diode-Clamped Converter for Photovoltaic Generators With Independent Voltage Control of Each Solar Array. IEEE Trans. Ind. Electron. 55 (7), 2713–2723.
Cacciato, M., Consoli, A., Attanasio, R., Gennaro, F., 2010. Soft-Switching Converter With HF Transformer for Grid-Connected Photovoltaic Systems. IEEE Trans. Ind. Electron. 57 (5), 1678–1686.
Cao, D., Jiang, S., Peng, F.Z., Li, Y., 2012. Low cost transformer isolated boost half-bridge micro-inverter for single-phase grid-connected photovoltaic system. In: 2012 Twenty-Seventh Annual IEEE Applied Power Electronics Conference and Exposition (APEC), Orlando, FL (pp. 71-78).
Carrasco, J.M., Franquelo, L.G., Bialasiewicz, J.T., Galvan, E., Guisado, R.C.P., Prats, M.A.M., Leon, J.I., Moreno-Alfonso, N., 2006. IEEE Trans. Ind. Electron. 53 (4), 1002–1016.
Cha, H., Chen, L., Ding, R., Tang, Q., Peng, F.Z., 2008. An alternative energy recovery clamp circuit for full-bridge PWM converters with wide ranges of input voltage. IEEE Trans. Power Electron. 23 (6), 2828–2837.
Chau K.T., Ching T.W., Chan C.C., 1996. Constant-frequency multi-resonant converter-fed DC motor drives. In: 22nd International Conference on Industrial Electronics, Control, and Instrumentation Proceedings of the 1996 IEEE IECON, 1, pp. 78–83.
Chen, J.-F., Chen, R.-Y., Liang, T.-J., 2008. Study and Implementation of a Single-Stage Current-Fed Boost PFC Converter With ZCS for High Voltage Applications. IEEE Trans. Power Electron 23 (1), 379–386.
Chu, C., Li, C., 2009. Analysis and design of a current-fed zero-voltage-switching and zero-current-switching CL-resonant push-pull dc-dc converter. IET Power Electron. 2 (4), 456–465.
Coppola, M., Di Napoli, F., Guerriero, P., Iannuzzi, D., Daliento, S., Del Pizzo, A., 2016. An FPGA-Based Advanced Control Strategy of a GridTied PV CHB Inverter. IEEE Trans. Power Electron. 31 (1), 806–816.
Daraban, S., Petreus, D., Morel, C., 2013, November. A novel global MPPT based on genetic algorithms for photovoltaic systems under the influence of partial shading. In: IECON 2013-39th Annual Conference of the IEEE Industrial Electronics Society (pp. 1490-1495). IEEE.
Dash, P., Kazerani, M., 2011. A multilevel current-source inverter based grid-connected photovoltaic system. In: North American Power Symposium, Boston, MA, pp. 1–6.
Dash, P.P., Kazerani, M., 2012. Harmonic Elimination in a Multilevel Current-Source Inverter-based grid-connected Photovoltaic System. In: IECON 2012 – 38th Annual Conference on IEEE Industrial Electronics Society, pp. 1001–1006.
Do, H.-L., 2012. Asymmetrical Full-bridge Converter With High-Voltage Gain. IEEE Trans. Power Electron 27 (2), 860–868.
Dobakhshari, S.S., Fathi, S.H., Banaiemoqadam, A., Moghani, J.S., 2016. A new current-fed high step-up quasi-resonant DC-DC converter with voltage quadrupler. In: 2016 7th Power Electronics and Drive Systems Technologies Conference (PEDSTC), pp. 197–202.
Dobakhshari, S.S., Milimonfared, J., Taheri, M., Moradisizkoohi, H., 2017. A Quasi-Resonant Current-Fed Converter With Minimum Switching Losses. IEEE Trans. Power Electron 32 (1), 353–362.
Elgendy, M.A., Zahawi, B., Atkinson, D.J., 2012. Assessment of the incremental conductance maximum power point tracking algorithm. IEEE Trans. Sustainable Energy 4 (1), 108–117.
Erickson, R.W., Hernandez, A.F., Witulski, A.F., Xu, R., 1989. A nonlinear resonant switch. In: 20th Annual IEEE Power Electronics Specialists Conference, (pp. 43–50). IEEE.
Farrington, R., Jovanovic, M.M., Lee, F.C., 1990. Constant-frequency zero-voltage-switched multi-resonant converters: analysis, design, and experimental results. In: 21st Annual IEEE Conference on Power Electronics Specialists, pp. 197–205.
Forouzesh, M., Siwakoti, Y.P., Gorji, S.A., Blaabjerg, F., Lehman, B., 2017. Step-Up DC–DC Converters: A Comprehensive Review of Voltage-Boosting Techniques, Topologies, and Applications. IEEE Trans. Power Electron. 32 (12), 9143–9178.
Fujii, K., Kikuchi, T., Koubayashi, H., Yoda, K., 2013. 1-mw advanced t-type npc converters for solar power generation system. In: 2013 15th European Conference on Power Electronics and Applications (EPE), 1-10.
Garcia, V., Rico, M., Sebastian, J., Hernando, M.M., Uceda, J., 1994. An optimized DC-to-DC converter topology for high-voltage pulse-load applications. In: Proceedings of 1994 Power Electronics Specialist Conference, pp. 1413–1421.
Gautam, D., Musavi, F., Edington, M., Eberle, W., Dunford,, W.G., 2011. An automotive on-board 3.3 kW battery charger for PHEV application. In: Proc. IEEE Vehicle Power Propulsion Conf, pp. 1–6.
Gilbert, A.J., Bingham, C.M., Stone, D.A., Foster, M.P., 2007. Normalized Analysis and Design of LCC Resonant Converters. IEEE Trans. Power Electron. 22 (6), 2386–2402.
Gnana Samdandam, K., Edpuganti, A., Rathore, A.K., Rodriguez, J., Srinivasan, D., 2019. Hybrid svm-sopwm modulation of current-fed three-level inverter for high power application. IEEE Trans. Ind. Appl. 55 (4), 4344–4358.
Gnanasambandam, K., Rathore, A.K., Edpuganti, A., Srinivasan, D., Rodriguez, J., 2017. Current-fed multilevel converters: An overview of circuit topologies, modulation techniques, and applications. IEEE Trans. Power Electron. 32 (5), 3382–3401.
Guedouani, R., Fiala, B., Berkouk, E., Boucherit, M., 2011. Modeling and control of multilevel three-phase PWM current source inverter. In: International Aegean Conference on Electrical Machines and Power Electronics and Electromotion, Joint Conference, pp. 455–460.
Harada K., Sakamoto H., 1990. Switched snubber for high frequency switching. In: 21st Annual IEEE Conference on Power Electronics Specialists, pp. 181–188.
Henze, C.P., Martin, H.C., Parsley, D.W., 1988. Zero-voltage switching in high frequency power converters using pulse width modulation. In: APEC '88 Third Annual IEEE Applied Power Electronics Conference and Exposition, pp. 33–40.
Hsieh, Y.-H., Lee, F.C., 2018. Accurate Small-Signal Modeling of Resonant Converter Based on Perturbation on the State Plane. In: 2018 IEEE Energy Conversion Congress and Exposition (ECCE) (pp. 6809–6816). IEEE.
Hsieh, Y.-H., Lee, F.C., 2018b. Modeling resonant converters in a rotating, polar coordinate. In: 2018 IEEE Applied Power Electronics Conference and Exposition (APEC). IEEE, pp. 938–943.
Hu, J., Joebges, P., Pasupuleti, G.C., Averous, N.R., De Doncker, R.W., 2019. A Maximum-Output-Power-Point-Tracking-Controlled Dual-Active Bridge Converter for Photovoltaic Energy Integration Into MVDC Grids. IEEE Trans. Energy Convers. 34 (1), 170–180.
Hu, Y., Cao, W., Finney, S.J., Xiao, W., Zhang, F., McLoone, S.F., 2014. New Modular Structure DC–DC Converter Without Electrolytic Capacitors for Renewable Energy Applications. IEEE Trans. Sustainable Energy 5 (4), 1184–1192.
Hu, Y., Xiao, W., Cao, W., Ji, B., Morrow, D.J., 2015. Three-Port DC–DC Converter for Stand-Alone Photovoltaic Systems. IEEE Trans. Power Electron. 30 (6), 3068–3076.
Ilic, M., Maksimovic, D., 2007. Phase-shifted full bridge DC-DC converter with energy recovery clamp and reduced circulating current. In: Proc. IEEE Appl. Power Electron. Conf. (APEC), Feb. 25–Mar. 1, (pp. 969–975).
Ilves, K., Antonopoulos, A., Norrga, S., Nee, H., 2012. Steady-state analysis of interaction between harmonic components of arm and line quantities of modular multilevel converters. IEEE Trans. Power Electron. 27 (1), 57–68.
Islam, S., Woyte, A., Belmans, R., Heskes, P., Rooij, P., Hogedoorn, M.R., 2006. Cost effective second generation AC-modules: Development and testing aspects. Energy. 31 (12), 1897–1920.
Islam, M.R., Mahfuz-Ur-Rahman, A.M., Islam, M.M., Guo, Y.G., Zhu, J.G., 2017. Modular medium-voltage grid-connected converter with improved switching techniques for solar photovoltaic systems. IEEE Trans. Ind. Electron. 64 (11), 8887–8896.
Isurin, A., Cook, A., 2001. A novel resonant converter topology and its application. In: 2001 IEEE 32nd Annual Power Electronics Specialists Conference (IEEE Cat. No.01CH37230) 2. pp. 1039–1044.
Ivensky, G., Kats, A., Ben-Yaakov, S., 1999. An RC load model of parallel and series-parallel resonant DC-DC converters with capacitive output filter. IEEE Trans. Power Electron. 14 (3), 515–521.
Jain, P.K., Kang, W., Soin, H., Xi, Y., 2002. Analysis and design considerations of a load and line independent zero voltage switching full bridge dc/dc converter topology. IEEE Trans. Power Electron. 17 (5), 649–657.
Jang, S., et al., 2007. Fuel cell generation system with a new active clamping current-fed

half-bridge converter. IEEE Trans. Energy Conversion. 22(2), 332.
Johnson, S.D., Witulski, A.F., Erickson, R.W., 1988. Comparison of resonant topologies in high-voltage DC applications". IEEE Trans. Aerosp. Electron. Syst. 24 (3), 263–274.
Jr H. C. M., 1986. Topology for miniature power supply with low voltage and low ripple requirements. US4618919A.
Kang, Y.-G., Upadhyay, A.K., Stephens, D.L., 1991. Mar. Analysis and design of a half-bridge parallel resonant converter operating above resonance. IEEE Trans. Ind. Appl. 27 (2), 386–395.
Kazimierczuk, M.K., Abdulkarim, A., 1995. Current-source parallel-resonant DC/DC converter. IEEE Trans. Ind. Electron. 42 (2), 199–208.
Killi, M., Samanta, S., 2015. Modified perturb and observe MPPT algorithm for drift avoidance in photovoltaic systems. IEEE Trans. Ind. Electron. 62 (9), 5549–5559.
Killi, M., Samanta, S., 2019. Voltage-Sensor-based MPPT for Stand-alone PV Systems through Voltage Reference Control. IEEE J. Emerg. Sel. Top. Power Electron. 7 (2), 1399–1407.
Kim, Y., Shin, S., Lee, J., Jung, Y., Won, C., 2014. Soft-Switching Current-Fed Push-Pull Converter for 250-W AC Module Applications. IEEE Trans. Power Electron. 29 (2), 863–872.
Kim, E., Kwon, B., 2009. High step-up resonant push-pull converter with high efficiency. IET Power Electron. 2 (1), 79–89.
Kim, J., Kim, M., Yeon, C., Moon, G., 2013. Analysis and design of Boost-LLC converter for high power density AC-DC adapter. In: 2013 IEEE ECCE Asia Downunder. IEEE, pp. 6–11.
Kouro, S., Malinowski, M., Gopakumar, K., Pou, J., Franquelo, L., Wu, B., Rodriguez, J., Perez, M., Leon, J., 2010. Recent Advances and Industrial Applications of Multilevel Converters. IEEE Trans. Ind. Electron. 57 (8), 2553–2580.
Kwon, J., Kim, E., Kwon, B., Nam, K., 2009a. High-Efficiency Fuel Cell Power Conditioning System With Input Current Ripple Reduction. IEEE Trans. Ind. Electron. 56 (3), 826–834.
Kwon, Jung-Min, et al., 2009b. High-efficiency fuel cell power conditioning system with input current ripple reduction. IEEE Trans. Ind. Electron. 56 (3), 826–834.
Larbes, C., Cheikh, S.A., Obeidi, T., Zerguerras, A., 2009. Genetic algorithms optimized fuzzy logic control for the maximum power point tracking in photovoltaic system. Renewable Energy 34 (10), 2093–2100.
Lashab, A., Sera, D., Guerrero, J.M., 2019. A Dual-Discrete Model Predictive Control-based MPPT for PV systems. IEEE Trans. Power Electron. 34 (10), 9686–9697.
Lee, C.Q., Siri, K., 1986. Analysis and Design of Series Resonant Converter by State-Plane Diagram. IEEE Trans. Aerosp. Electron. Syst. 22 (6), 757–763.
Leedy, A.W., Guo, L., Aganah, K.A., 2012. March. A constant voltage MPPT method for a solar powered boost converter with DC motor load. In: 2012 Proceedings of IEEE Southeastcon. IEEE, pp. 1–6.
Leung, Andrew SW, Chung, Henry SH, Chan, Tony, 2007. A ZCS isolated full-bridge boost converter with multiple inputs. In: Proc. IEEE Power Electronics Specialists Conference (PESC), pp. 2542–2548.
Lin, B.R., Lin, Y., 2019. Parallel current-fed resonant converter with balance current sharing and no input ripple current. IET Power Electron. 12 (2), 212–219.
Lin, W.M., Hong, C.M., Chen, C.H., 2011. Neural-network-based MPPT control of a stand-alone hybrid power generation system. IEEE Trans. Power Electron. 26 (12), 3571–3581.
Liu, B., Duan, S., Cai, T., 2011. Photovoltaic DC-Building-Module-Based BIPV System—Concept and Design Considerations. IEEE Trans. Power Electron. 26 (5), 1418–1429.
Liu, F., Duan, S., Liu, F., Liu, B., Kang, Y., 2008. A variable step size INC MPPT method for PV systems. IEEE Trans. Ind. Electron. 55 (7), 2622–2628.
Liu, J., Zheng, Z., Wang, K., Li, Y.D., 2019. Comparison of boost and LLC converter and active clamp isolated full-bridge boost converter for photovoltaic DC system. The Journal of Engineering. 16, 3007–3011.
Liu, K.-H., Lee, F.C.Y., 1990. Jul. Zero-voltage switching technique in DC/DC converters. IEEE Trans. Power Electron. 5 (3), 293–304.
Liu, L.-H., Lee, F.C., 1984. Resonant Switches - A Unified Approach to Improve Performances of Switching Converters. In: IN[TEL]EC '84 - International Telecommunications Energy Conference. IEEE, pp. 344–351.
Liu, Y.H., Huang, S.C., Huang, J.W., Liang, W.C., 2012. A particle swarm optimization-based maximum power point tracking algorithm for PV systems operating under partially shaded conditions. IEEE Trans. Energy Convers. 27 (4), 1027–1035.
Lizana, R., Perez, M.A., Bernet, S., Espinoza, J.R., Rodriguez, J., 2016. Control of arm capacitor voltages in modular multilevel converters. IEEE Trans. Power Electron. 31, 1774–1784.
Lopez-Lapena, O., Penella, M.T., 2012. Low-power FOCV MPPT controller with automatic adjustment of the sample&hold. Electron. Lett. 48 (20), 1301–1303.
Sivakumar, M.R.A., 2015.A. Fault-Tolerant Single-Phase Five-Level Inverter for Grid-Independent PV Systems. IEEE Trans. Ind. Electron. 62 (12), 7569–7577.
Mahmoud, Y., El-Saadany, E.F., 2016. A novel MPPT technique based on an image of PV modules. IEEE Trans. Energy Convers. 32 (1), 213–221.
Maksimovic, D., Cuk, S., 1991. A general approach to synthesis and analysis of quasi-resonant converters. IEEE Trans. Power Electron. 6 (1), 127–140.
Martin-Ramos, J.A., Diaz, J., Pernia, A.M., Lopera, J.M., Nuno, F., 2007. Dynamic and Steady-State Models for the PRC-LCC Resonant Topology With a Capacitor as Output Filter. IEEE Trans. Ind. Electron. 54 (4), 2262–2275.
Martin-Ramos, J.A., Pernia, A.M., Diaz, J., Nuno, F., Martinez, J.A., 2008. Power supply for a high-voltage application. IEEE Trans. Power Electron. 23 (4), 1608–1619.
McMurray,W., 1971. Fast response stepped-wave switching power converter circuit. U.S. Patent 3 581 212.
Mei, J., Xiao, B., Shen, K., Tolbert, L.M., Zheng, J.Y., 2013. Modular multilevel inverter with new modulation method and its application to photovoltaic grid-connected generator. IEEE Trans. Power Electron. 28 (11), 5063–5073.
Metry, M., Shadmand, M.B., Balog, R.S., Abu-Rub, H., 2016. MPPT of photovoltaic systems using sensorless current-based model predictive control. IEEE Trans. Ind. Appl. 53 (2), 1157–1167.
Mohanty, S., Subudhi, B., Ray, P.K., 2015. A new MPPT design using grey wolf optimization technique for photovoltaic system under partial shading conditions. IEEE Trans. Sustainable Energy 7 (1), 181–188.
Mohanty, S., Subudhi, B., Ray, P.K., 2016. A grey wolf-assisted perturb & observe MPPT algorithm for a PV system. IEEE Trans. Energy Convers. 32 (1), 340–347.
Morten, Nymand, Andersen, Michael AE, 2010. High-efficiency isolated boost DC–DC converter for high-power low-voltage fuel-cell applications. IEEE Trans. Ind. Electron. 57 (2), 505–514.
Mousavi, A., Das, P., Moschopoulos, G., 2012. A Comparative Study of a New ZCS DC–DC Full-Bridge Boost Converter With a ZVS Active-Clamp Converter. IEEE Trans. Power Electron. 27 (3), 1347–1358.
Mweene, L.H., Wright, C.A., Schlecht, M.F., 1991. A 1 kW 500 kHz front-end converter for a distributed power supply system. IEEE Trans. Power Electron. 6 (3), 398–407.
Nabae, A., Takahashi, I., Akagi, H., New Neutral-Point-Clamped, A., Inverter, P.W.M., 1981. IEEE Trans. Ind. Appl. IA-17 (5), 518–523.
Nademi, H., Das, A., Burgos, R., Norum, L.E., 2016. A new circuit performance of modular multilevel inverter suitable for photovoltaic conversion plants. IEEE J. Emerg. Sel. Top. Power Electron. 4 (2), 393–404.
Nuno, F., Diaz, J., Sebastian, J., Lopera, J., 1992. A unified analysis of multi-resonant convertersPESC '92. In: Record. 23rd Annual IEEE Power Electronics Specialists Conference. IEEE, pp. 822–829.
Oruganti, R., Lee, F.C., 1985a. Resonant Power Processors, Part II-Methods of Control. IEEE Trans. Ind. Appl. 21 (6), 1461–1471.
Oruganti, R., Lee, F.C., 1985b. Resonant Power Processors, Part I—State Plane Analysis. IEEE Trans. Ind. Appl. 21 (6), 1453–1460.
Outeiro, M.T., Buja, G., Czarkowski, D., 2016. Resonant Power Converters: An Overview with Multiple Elements in the Resonant Tank Network IEEE Ind. Electron. Mag. 10 (2), 21–45.
Park Chansoo, Choi S., Lee Jeong-min, 2012. Quasi-resonant boost-half-bridge converter with reduced turn-off switching losses for 16V fuel cell application. In: Proceedings of the 7th International Power Electronics and Motion Control Conference, 3, pp. 1960–1964.
Park, K.-B., Moon, G.-W., Youn, M.-J., 2012. High Step-up Boost Converter Integrated With a Transformer-Assisted Auxiliary Circuit Employing Quasi-Resonant Operation. IEEE Trans. Power Electron 27 (4), 1974–1984.
Patii, D., Rathore, A.K., Srinivasan, D., Panda, S. K., 2014. High-frequency soft-switching LCC resonant current-fed DC/DC converter with high voltage gain for DC microgrid application. In: IECON 2014 - 40th Annual Conference of the IEEE Industrial Electronics Society, pp. 4293–4299. IEEE.
Pitel, I. J., 1986. Phase-Modulated Resonant Power Conversion Techniques for High-Frequency Link Inverters. IEEE Trans. Ind. Appl. 22(6), 1044–1051.
Prasanna, U.R., Rathore, A.K., Mazumder, S.K., 2013. Novel zero-current-switching current-fed half-bridge isolated DC/DC converter for fuel-cell-based applications. IEEE Trans. Ind. Appl. 49 (4), 1658–1668.
Prasanna, U.R., Rathore, A.K., 2013. Analysis, Design, and Experimental Results of a Novel Soft-Switching Snubberless Current-Fed Half-Bridge Front-End Converter-Based PV Inverter. IEEE Trans. Power Electron. 28 (7), 3219–3230.
Pan, X., Li, H., Liu, Y., Zhao, T., Ju, C., Rathore, A.K., 2020. An Overview and Comprehensive Comparative Evaluation of Current-Fed-Isolated-Bidirectional DC/DC Converter. IEEE Trans. Power Electron. 35 (3), 2737–2763.
Ranganathan, V.T., Ziogas, P.D., Stefanovic, V.R., 1982. A Regulated DC-DC Voltage Source Converter Using a High Frequency Link. IEEE Trans. Ind. Appl. 18 (3), 279–287.
Rathore, A.K., Patil, D.R., Srinivasan, D., 2016. Mar. Non-isolated Bidirectional Soft-Switching Current-Fed LCL Resonant DC/DC Converter to Interface Energy Storage in DC Microgrid. IEEE Trans. Ind. Appl. 52 (2), 1711–1722.
Rathore, Akshay K., Bhat, Ashoka K.S., Oruganti, Ramesh, 2012. Analysis, design and experimental results of wide range ZVS active-clamped LL type current-fed DC/DC converter for fuel cells to utility interface. IEEE Trans. Ind. Electron. 59 (1), 473–485.
Rodriguez, J., Bernet, S., Bin, W., Pontt, J.O., Kouro, S., 2007. Multilevel Voltage-Source-Converter Topologies for Industrial Medium-Voltage Drives. IEEE Trans. Ind. Electron. 54 (6), 2930–2945.
Rong, F., Gong, X., Huang, S., 2017. A novel grid-connected pv system based on mmc to get the maximum power under partial shading conditions. IEEE Trans. Power Electron. 32 (6), 4320–4333.
Rooij, Michael Andrew de, J. S. G., Mayer, Oliver Gerhard, EI-Barbari, Said Farouk Said, 2010. Quasi-AC, Photovoltaic Module for unfolder Photovoltaic Inverter. United States Patent US2010/0071742 A1.
Ryan, M.J., Brumsickle, W.E., Divan, D.M., Lorenz, R.D., 1998. A new ZVS LCL-resonant push-pull DC-DC converter topology. IEEE Trans. Ind. Appl. 34 (5), 1164–1174.
Sabate, J.A., Vlatkovic, V., Ridley, R.B., Lee, F.C., Cho, B.H., 1990. Design considerations for high-voltage high-power full-bridge zero-voltage switched PWM converter. Proc. Appl. Power Electron. Conf. (APEC) 275–284.
Sabate, J.A., Lee, F.C.Y., 1991. Offline application of the fixed-frequency clamped-mode series resonant converter. IEEE Trans. Power Electron. 6 (1), 39–47.
Sabate, J. A., Vlatkovic,V., Ridley,R. B. , Lee, F. C. , 1991. High-voltage, high power, ZVS, full-bridge PWM converter employing an active snubber, in Proc. 6th Annu, Appl. Power Electron. Conf. Expo., Dallas, TX, Mar.10–15, (pp. 158–163).
Sahoo, M., Keerthipati, S., 2017. A three-level lc-switching-based voltage boost npc inverter. IEEE Trans. Ind. Electron. 64 (4), 2876–2883.
Sasmal, T.S., Sensarma, P., 2018. A New Current Source based Resonant Tank for Switch Stress Reduction in DC-DC Converter. In: 2018 IEEE International Conference on Power Electronics, Drives and Energy Systems (pp. 1–6). IEEE.

Schlecht, M.F., Casey, L.F., 1988. Jan. Comparison of the square-wave and quasi-resonant topologies. IEEE Trans. Power Electron. 3 (1), 83–92.
Serban, E., Ordonez, M., Pondiche, C., 2015. Dc-bus voltage range extension in 1500 v photovoltaic inverters. IEEE J. Emerg. Sel. Top. Power Electron. 3 (4), 901–917.
Sewell, H.I., Foster, M.P., Bingham, C.M., Stone, D.A., Hente, D., Howe, D., 2003. Analysis of voltage output LCC resonant converters, including boost mode operation. IEE Proc.-Electric Power Appl. 150 (6), 673–679.
Seyedmahmoudian, M., Soon, T.K., Horan, B., Ghandhari, A., Mekhilef, S., Stojcevski, A., 2019. New ARMO-based MPPT Technique to Minimize Tracking Time and Fluctuation at Output of PV Systems under Rapidly Changing Shading Conditions. IEEE Trans. Ind. Inf.
Shafiei, N., Pahlevaninezhad, M., Farzanehfard, H., Motahari, S.R., 2011. Analysis and Implementation of a Fixed-Frequency LCLC Resonant Converter With Capacitive Output Filter. IEEE Trans. Ind. Electron. 58 (10), 4773–4782.
Shang, F., Niu, G., Krishnamurthy, M., 2017. March. Design and Analysis of a High-Voltage-Gain Step-Up Resonant DC–DC Converter for Transportation Applications. IEEE Trans. Transp. Electrif. 3 (1), 157–167.
Sharma, R., Das, A., 2019. Enhanced active power balancing capability of grid connected solar pv fed cascaded h-bridge converter. IEEE J. Emerg. Sel. Top. Power Electron. 7 (4), 2281–2291.
Sree, K.R., Rathore, A.K., 2015. Impulse Commutated Zero-Current Switching Current-Fed Push-Pull Converter: Analysis, Design, and Experimental Results. IEEE Trans. Ind. Electron 62 (1), 363–370.
Sree, K.R., Rathore, A.K., 2016. Impulse-Commutated Zero-Current-Switching Current-Fed Three-Phase DC/DC Converter. IEEE Trans. Ind. Appl 52 (2), 1855–1864.
Sree, K.R., Rathore, A.K., 2017a. Analysis and Design of Impulse-Commutated Zero-Current-Switching Single-Inductor Current-Fed Three-Phase Push-Pull Converter. IEEE Trans. Ind. Appl 53 (2), 1517–1526.
Sree, K.R., Rathore, A.K., 2017b. Impulse Commutated High-Frequency Soft-Switching Modular Current-Fed Three-Phase DC/DC Converter for Fuel Cell Applications. IEEE Trans. Ind. Electron 64 (8), 6618–6627.
Steigerwald, R.L., 1984. High-Frequency Resonant Transistor DC-DC Converters. IEEE Trans. Ind. Electron. 31 (2), 181–191.
Steigerwald, R.L., 1988. A comparison of half-bridge resonant converter topologies. IEEE Trans. Power Electron. 3 (2), 174–182.
Stonier, A.A., Lehman, B., 2018. An intelligent-based fault-tolerant system for solar-fed cascaded multilevel inverters. IEEE Trans. Energy Convers. 33 (3), 1047–1057.
Sun, W., Xing, Y., Wu, H., Ding, J., 2018. Modified High-Efficiency LLC Converters With Two Split Resonant Branches for Wide Input-Voltage Range Applications. IEEE Trans. Power Electron. 33 (9), 7867–7879.
Tabisz, W.A., Lee, F.C.Y., 1989a. Zero-voltage-switching multiresonant technique-a novel approach to improve performance of high-frequency quasi-resonant converters. IEEE Trans. Power Electron. 4 (4), 450–458.
Tabisz, W.A., Lee, F.C., 1989. DC analysis and design of zero-voltage-switched multi-resonant converters. In: 20th Annual IEEE Power Electronics Specialists Conference (pp. 243–251). IEEE.
Tabisz, W.A., Lee, F.C., 1991. Principles of quasi- and multi-resonant power conversion techniques. In: 1991 IEEE International Sympoisum on Circuits and Systems (pp. 1053–1056), IEEE.
Tan, X., Ruan, X., 2016. Equivalence Relations of Resonant Tanks: A New Perspective for Selection and Design of Resonant Converters. IEEE Trans. Ind. Electron. 63 (4), 2111–2123.
Tarzamni, H., Babaei, E., Gharehkoushan, A.Z., 2017. A Full Soft-Switching ZVZCS Flyback Converter Using an Active Auxiliary Cell. IEEE Trans. Ind. Electron 64 (2), 1123–1129.
Thrimawithana, D.J., Madawala, U.K., 2008. Analysis of Split-Capacitor Push-Pull Parallel-Resonant Converter in Boost Mode. IEEE Trans. Power Electron. 23 (1), 359–368.
Tian, S., Lee, F.C., Li, Q., 2016. Equivalent circuit modeling of LLC resonant converter. In: 2016 IEEE Applied Power Electronics Conference and Exposition (APEC) (pp. 1608–1615). IEEE.
Tsai, F.-S., Lee, F.C., 1988. A complete DC characterization of a constant-frequency, clamped-mode, series-resonant converter. In: PESC '88 Record, 19th Annual IEEE Power Electronics Specialists Conference (pp. 987–996).
Tsai, F.-S., Sabate, J., Lee, F. C., 1989. Constant-frequency, zero-voltage-switched, clamped-mode parallel-resonant converter. In: Conference Proceedings, Eleventh International Telecommunications Energy Conference, (pp. 16.4/1-16.4/7).
Tsai, Fu-Sheng, Materu, P., Lee, F.C.Y., 1988. Constant-frequency clamped-mode resonant converters. IEEE Trans. Power Electron. 3(4), 460–473.
Vakacharla, V.R., Kumar Rathore, K., 2019. Performance Evaluation of LLC-SRC and LCC-T Resonant Tanks in Low-Voltage High-Current applications. In: 2019 IEEE 28th International Symposium on Industrial Electronics (ISIE) (pp. 2091–2096). IEEE.
Vakacharla, V.R., Rathore, A.K., 2019b. Apr. Current-Fed Isolated LCC-T Resonant Converter With ZCS and Improved Transformer Utilization. IEEE Trans. Ind. Electron. 66 (4), 2735–2745.
Vakacharla, V.R., Rathore, K., 2019c. Sep. Isolated Soft Switching Current Fed LCC-T Resonant DC–DC Converter for PV/Fuel Cell Applications. IEEE Trans. Ind. Electron. 66 (9), 6947–6958.
Vakacharla, V.R., Kumar Rathore, K., 2018. Performance Evaluation of LLC-SRC and LCC-T Resonant Tanks in Low-Voltage High-Current applications. In: 2019 IEEE 28th International Symposium on Industrial Electronics (ISIE) (pp. 2091–2096). IEEE.
Vakacharla, V.R., Rathore, A.K., Sahoo, S.K., 2018. Modeling and experimental verification of LCC-T resonant converter. In: 2018 IEEE International Conference on Power Electronics, Drives and Energy Systems (PEDES). IEEE, pp. 1–6.
Vekhande, V., Kothari, N., Fernandes, B.G., 2015. Switching State Vector Selection Strategies for Paralleled Multilevel Current-Fed Inverter Under Unequal DC-Link Currents Condition. IEEE Trans. Power Electron. 30 (4), 1998–2009.
Verghese, G.C., Elbuluk, M.E., Kassakian, J.G., 1986. Apr. A General Approach to Sampled-Data Modeling for Power Electronic Circuits. IEEE Trans. Power Electron. 1 (2), 76–89.
Villanueva, E., Correa, P., Rodriguez, J., Pacas, M., 2009. Control of a single-phase cascaded h-bridge multilevel inverter for grid-connected photovoltaic systems. IEEE Trans. Ind. Electron. 56 (11), 4399–4406.
Vishal, A.A.G., Basu, K., Gurunathan, R., 2018. Resonance based Current-fed Isolated DC/DC Converter for High Voltage Applications. In: 2018 IEEE International Conference on Power Electronics, Drives and Energy Systems. IEEE, pp. 1–6.
Vorperian, V., Cuk, S., 1983. Small signal analysis of resonant converters. In: 1983 IEEE Power Electronics Specialists Conference. IEEE, pp. 269–282.
Vorperian, V., Cuk, S., 1982. A complete DC analysis of the series resonant converter. In: IEEE Power Electronics Specialists Conference, pp. 85–100.
Walker, G.R., Sernia, P.C., 2004. Cascaded DC-DC converter connection of photovoltaic modules. IEEE Trans. Power Electron. 19 (4), 1130–1139.
Wang, C., Xu, S., Lu, S., Sun, W., 2016. An accurate design method of RCD circuit for flyback converter considering diode reverse recovery. In: 2016 IEEE International Conference on Industrial Technology (ICIT), pp. 269–274.
Wang, H., Kou, L., Liu, Y., Sen, P.C., 2017. A new six-switch five-level active neutral point clamped inverter for pv applications. IEEE Trans. Power Electron. 32 (9), 6700–6715.
Wang, Huai, et al., 2009. A ZCS current-fed full-bridge PWM converter with self-adaptable soft-switching snubber energy. IEEE Trans. Power Electron. 24 (8), 1977–1991.
Xinke, Wang, Xiaogao, X., Chen, Z., Zhaoming, Q., Rongxiang, Z., 2008. Low voltage and current stress ZVZCS full bridge DC–DC converter using center tapped rectifier reset. IEEE Trans. Ind. Electron. 55 (3), 1470–1477.
Watson R., Hua G. C., Lee F. C., 1994. Characterization of an active clamp flyback topology for power factor correction applications. In: Proceedings of 1994 IEEE Applied Power Electronics Conference and Exposition - ASPEC'94, 1, pp. 412–418.
Watson, R., Lee, F.C., Hua, G.C., 1996. Utilization of an active-clamp circuit to achieve soft switching in flyback converters. IEEE Trans. Power Electron 11 (1), 162–169.
Wijeratne, D.S., Moschopoulos, G., 2014. A ZVS-PWM Full-Bridge Converter With Reduced Conduction Losses. IEEE Trans. Power Electron. 29 (7), 3501–3513.
Wolfs, P.J., 1993. A current-sourced DC-DC converter derived via the duality principle from the half-bridge converter. IEEE Trans. Ind. Electron. 40 (1), 139–144.
Wu, Q., Wang, Q., Xu, J., Li, H., Xiao, L., 2017. A High-Efficiency Step-Up Current-Fed Push-Pull Quasi-Resonant Converter With Fewer Components for Fuel Cell Application. IEEE Trans. Ind. Electron. 64 (8), 6639–6648.
Wu, T.F., Chen, Y.C., Yang, J.G., Kuo, C.L., 2010. Isolated bidirectional full-bridge DC–DC converter with a flyback snubber. IEEE Trans. Power Electron. 25 (7), 1915–1922.
Wu, T.-F., Chen, Y.-K., Yang, C.-H, and Liang, S.-A., 1999. A structural approach to synthesizing and analyzing quasi-resonant and multi-resonant converters. In: 30th Annual IEEE Power Electronics Specialists Conference (pp. 1024–1029). IEEE.
Wu, Tsai-Fu, et al., 2008. An active-clamp push–pull converter for battery sourcing applications. IEEE Trans. Ind. Appl. 44 (1), 194–204.
Wu, X., Zhang, J., Xie, X., Qian, Z., 2006. Analysis and optimal design considerations for an improved full bridge ZVS dc-dc converter with high efficiency. IEEE Trans. Power Electron. 21 (5), 1225–1233.
Xue, L., Zhang, J., 2018. Highly Efficient Secondary-Resonant Active Clamp Flyback Converter. IEEE Trans. Ind. Electron 65 (2), 1235–1243.
Xuewei, P., Rathore, A.K., 2014. Novel bidirectional snubberless naturally commutated soft-switching current-fed full-bridge isolated DC/DC converter for fuel cell vehicles. IEEE Trans. Ind. Electron. 61 (5), 2307–2315.
Yang, Bo, Lee, F. C., Zhang, A. J., Huang, Guisong, 2002. LLC resonant converter for front end DC/DC conversion. In: APEC. Seventeenth Annual IEEE Applied Power Electronics Conference and Exposition (Cat. No.02CH37335) (pp. 1108–1112).
Yang, E.X., Lee, F.C., Jovanovic, M.M., 1992. Small-signal modeling of series and parallel resonant converters. In: (Proceedings) APEC '92 Seventh Annual Applied Power Electronics Conference and Exposition (pp. 785–792). IEEE.
York, B., Yu, W., Lai, J.-S., 2013. An Integrated Boost Resonant Converter for Photovoltaic Applications. IEEE Trans. Power Electron. 28 (3), 1199–1207.
Yoshida, K., Ishii, T., Nagagata, N., 1992. Zero voltage switching approach for flyback converter. In: Fourteenth International Telecommunications Energy Conference - IN^{TEL}EC '92, pp. 324–329.
Yu, S.-Y., Chen, R., Viswanathan, A., 2018, "Survey of Resonant Converter Topologies," p. 26.
Yu, Y., Konstantinou, G., Townsend, C.D., Aguilera, R.P., Agelidis, V.G., 2017. Delta-connected cascaded h-bridge multilevel converters for large-scale photovoltaic grid integration. IEEE Trans. Ind. Electron. 64 (11), 8877–8886.
Yu, Y., Konstantinou, G., Hredzak, B., Agelidis, V.G., 2016. Power balance optimization of cascaded h-bridge multilevel converters for largescale photovoltaic integration. IEEE Trans. Power Electron. 31 (2), 1108–1120.
Yu, Y., Konstantinou, G., Hredzak, B., Agelidis, V.G., 2015. Operation of Cascaded H-Bridge Multilevel Converters for Large-Scale Photovoltaic Power Plants Under Bridge Failures. IEEE Trans. Ind. Electron. 62 (11), 7228–7236.
Yuan, B., Yang, X., Li, D., 2010. A high efficiency current fed multi-resonant converter for high step-up power conversion in renewable energy harvesting. In: 2010 IEEE Energy Conversion Congress and Exposition, pp. 2637–2641.
Zakzouk, N.E., Elsaharty, M.A., Abdelsalam, A.K., Helal, A.A., Williams, B.W., 2016. Improved performance low-cost incremental conductance PV MPPT technique. IET Renew. Power Gener. 10 (4), 561–574.
Zeng, Jianhong, Ying, Jianping, Zhang, Qingyou, 2002. A novel DC/DC ZVS converter for battery input application. In: APEC Seventeenth Annual IEEE Applied Power Electronics Conference and Exposition (Cat. No.02CH37335) 2. pp. 892–896.
Zhang, J., Huang, X., Wu, X., Qian, Z., 2010. A High Efficiency Flyback Converter With New Active Clamp Technique. IEEE Trans. Power Electron. 25 (7), 1775–1785.

Zhang, Xing-Zhu, Huang, Shi-Peng, 1991. Novel high frequency quasi-square-wave converter topologies. In: Thirteenth International Telecommunications Energy Conference - INTELEC 91 (pp. 663–667). IEEE.
Zheng, W., Ming, C., Yongqiang, L., Shichuan, D., 2011. Active damping of LC resonance for interleaved CSC fed motor drives. In: 2011 International Conference on Electrical Machines and Systems, Beijing, pp. 1–6.
Yin, Y., Liu, J., Sanchez, J.A., Wu, L., Vazquez, S., Leon, J.I., Franquelo, L.G., 2019. Observer-based adaptive sliding mode control of NPC converters: An RBL neural network approach. IEEE Trans. Power Electron. 34 (4), 3831–3841.
Xu, D., Liu, J., Yan, X.G., Yan, W., 2018. A novel adaptive neural network constrained control for a multi-area interconnected power system with hybrid energy storage. IEEE Trans. Ind. Electron. 65 (8), 6625–6634.

Further reading

Radha, S.K., Rathore, A.K., 2016. Comparison and evaluation of three-phase current-fed impulse commutated ZCS DC/DC converter topologies with variable frequency modulation. In: 2016 IEEE Uttar Pradesh Section International Conference on Electrical, Computer and Electronics Engineering (UPCON), Varanasi, pp. 641–646.